BULLETIN 46

Topical Study of Lead-Zinc Gossans

by WILLIAM C. KELLY

Field and laboratory studies of lead-zinc ore outcrops, mineralogy of gossan limonite, outcrop colors and porosity, with a discussion of nonsulfide boxwork structures

1958

STATE BUREAU OF MINES AND MINERAL RESOURCES
NEW MEXICO INSTITUTE OF MINING & TECHNOLOGY
CAMPUS STATION SOCORRO, NEW MEXICO

NEW MEXICO INSTITUTE OF MINING & TECHNOLOGY E. J. Workman, *President*

STATE BUREAU OF MINES AND MINERAL RESOURCES
Alvin J. Thompson, *Director*

THE REGENTS

MEMBERS EX OFFICIO

The Honorable Edwin L. Mechem ..... *Governor of New Mexico*

Mrs. Georgia L. Lusk ..... *Superintendent of Public Instruction*

APPOINTED MEMBERS

Robert W. Botts ..... Albuquerque

Holm 0. Bursum, Jr. ..... Socorro

Thomas M. Cramer ..... Carlsbad

John N. Mathews, Jr. ..... Socorro

Richard A. Matuszeski ..... Albuquerque

Contents

Illustrations

TABLES **Page**

FIGURES

PLATES

Abstract

The reconstruction of lead-zinc ores from their leached outcrops is a problem fundamental to the discovery of new deposits in areas where climate is favorable to the development of gossan. Several approaches to this problem were selected and studied in the field and laboratory.

X-ray studies and differential thermal analyses of 159 gossan "limonites" (transported and indigenous) indicate that goethite is the predominant ferric oxide monohydrate in leached lead-zinc outcrops. Lepidocrocite is either extremely rare or completely absent. The predominance of goethite can be explained in terms of the chemical conditions under which the mineral has been synthesized in the laboratory. Rather than revealing new outcrop criteria of use in the search for ores, the application of thermal analysis to gossan "limonites" showed that this technique is not, as formerly thought, a reliable means for identifying the hydrous ferric oxide minerals. Thermal curves closely resembling published standards for (a) goethite, (b) lepidocrocite, and (c) goethite-lepidocrocite mixtures may be produced by goethite alone, depending on the degree of crystallization in the materials tested.

The application of boxwork structures as surface guides to ore is reviewed, and a number of "nonsulfide" boxworks observed in the field are described. The latter may be sufficiently similar to true sulfide derivatives to cause some confusion regarding the nature of the original materials before oxidation; hence their recognition at the surface is a matter of practical importance. It is also important that a distinction be made between hypogene and supergene "boxwork siderites." The super-gene boxworks originate and occur in limestones beneath oxidizing ore, and if they are exposed at the surface erosion, they would indicate removal of overlying ore rather than the possible existence of workable ore below the outcrops. Hypogene boxworks do not convey the same meaning, since they cannot be expected to bear as definite a spacial relationship to ore.

Eh-pH diagrams prepared for the system $Fe\text{-}H_2O\text{-}0O_2\text{-}S$ in the oxide zone define semiquantitatively the chemical conditions under which siderite is to be expected as the stable precipitate in the country rock below actively oxidizing ore. These calculations lend support to Locke's tentative observation that siderite precipitates in saturated ground, and limonite in more aerated material. The formation of siderite rather than limonite in the ground below ore would be favored, but not exclusively controlled, by the presence of cuprous ion in the descending solutions.

The quantitative relationship between gossan porosity and leached-sulfide volumes was also investigated. A technique involving the application of microscopic counts to the measurement of cavities after sulfides was developed, which, in some cases, will permit direct estimates of the

volume of sulfides originally contained by a given gossan sample. This technique is applicable only to outcrops in which voids after sulfides can be clearly distinguished from nonsulfide cavities.

Even in cases of "ideal gossans" in which there appears to be excellent cavity reproduction of former sulfides, gossan porosity determinations made by standard weighing procedures are of little value because (1) the quantity of pores in the original unoxidized ore is unknown from data available at the surface, (2) leaching of nonsulfide (gangue) minerals may increase porosity in the outcrop, and (3) gossan pores may be coated or even sealed by limonite, silica, gypsum, or the metal oxysalts.

Outcrop colors that could be related to specific original sulfides were recorded with the help of a standard color chart in each of the mining districts visited. In this study, the colors of iron precipitates in leached lead-zinc outcrops were found to be of very definite local value as criteria of specific primary sulfides. However, no one gossan color or color pattern was noted as universally diagnostic of the former presence of pyrite, galena, or sphalerite. Factors other than original sulfides which may affect the colors seen in a leached outcrop are manifold; in view of this, the lack of general color criteria is understandable.

Introduction

BACKGROUND, SCOPE, AND PURPOSE

Some 30 years have passed since the publication of Augustus Locke's creative volume on "leached outcrops as guides to copper ore" (1926). This new approach to the search for ores stimulated many constructive studies in the late twenties and early thirties, some of which found their way into print. Regrettably, however, the results of most such studies seem to have been buried in the files of exploration companies. The subsequent investigations of Locke and of his associates Roland Blanchard and **P.** F. Boswell furnish exceptions, for which the mining geologist working in climates favorable to the development of gossan should be profoundly grateful.

Since the publication of the early works of these three authors, very few papers have appeared which have had as their purpose the development of criteria applicable to ore interpolation at depth. Meantime, the need for definite outcrop guides to the reconstruction of leached ores has increased enormously. Large sections of the world northern Mexico, for example — are areas of gossan occurrence in which the outcrops have been examined in no more than cursory fashion by competent geologists. It is probably fair to say that the greatest immediate promise for finding new sulfide ore bodies lies in the application of mineralogic or geochemical techniques of study to such outcrops.

It was with this thought in mind that the writer began in the summer of 1951 a reexamination of available data on gossans. Several lines of investigation suggested themselves for determining "from above," as it were, the relation between primary ores and their oxidized products. Thermal analysis was applied to many samples of gossan limonite to determine whether variations in the proportions of goethite and lepidocrocite might reflect differences in the primary source of the iron oxide minerals. The quantitative relationship between gossan porosity and the original volume of leached sulfides was studied by measurement of sulfide volumes and capping porosities in a number of ore bodies. Detailed notes were taken on outcrop colors in each area studied, to establish any general color criteria that might be of value to the prospector. Boxwork structures were studied wherever seen, and a section of this bulletin will be devoted to a discussion of a number of the nonsulfide boxworks commonly found in several localities.

In the field, the approach was chiefly through study of ore bodies that could be traced continuously from the sulfide zone up into oxidized ore at the surface. Shallow sulfide ore offers the best facsimile of the original ore in an outcrop even though, as stressed by earlier workers in this field, there is never certainty that ore formerly existing in the plane of the surface was similar to present-day ore beneath the leached

outcrops. The correlation of primary ore and gossan was stressed, therefore, in the selection of areas for this study.

At the start, the writer was faced with the choice of making either an exhaustive study of all phases of oxidation in a single mining area, or a broader study of selected aspects of the leached-outcrop problem applied to many areas of varied geologic and climatic setting. The latter course was selected because it offered grounds for generalization on a larger scale.

To avoid the complications introduced by the presence of chalcopyrite in a mixed sulfide deposit, attention has been focused on ores high in lead and zinc, but low in copper. In this way, it became unnecessary to cope with the problem of mixed pyrite-chalcopyrite sources for iron precipitates at the surface. Limonites in leached outcrops could be assigned to gangue minerals, pyrite, or marmatite as primary iron sources, thus eliminating one variable from the start.

The first field season (1951) was devoted to study of several lead-zinc deposits in southwestern New Mexico. In 1952, the research was continued in New Mexico and extended to northern Mexico, and terminated with an examination of deposits in the East Tennessee zinc district. The final field season went into an investigation of lead-zinc deposits in and around the Bingham district in Utah. Throughout this period, several mines in the Northeastern United States were visited to gain familiarity with typical oxidized deposits in a glaciated region of moderately heavy rainfall unfavorable to the formation of gossan.

In the organization of this bulletin, brief descriptions of sample-areas have been set apart from text dealing with the various approaches to the leached outcrop problem. The hope has been to emphasize new data on gossans rather than to scatter such data through a text of regional descriptions.

This is the first in a series of oxidation studies being carried out by students in the Ore Genesis Laboratory at Columbia University under the able direction of Professor Charles H. Behre, Jr.

The present study was submitted for publication to the New Mexico Institute of Mining and Technology in October 1954. The manuscript was revised in August 1957. The author regrets that the study was in press before the publication of the important article by N. K. Huber on the Eh-pH relations of the iron minerals (Econ. Geol., v. 58, p. 123, March-April 1958).

Acknowledgments

I wish to acknowledge the sponsorship given to this project by the New Mexico Bureau of Mines and Mineral Resources, and to thank its former director, Dr. Eugene Callaghan, and its present director, Mr. Alvin J. Thompson, for their kind and helpful support.

All phases of this work were directed by Professor Charles H. Behre, Jr., of Columbia University. His understanding of the problems involved in a study such as this and his guidance over difficult ground proved a constant source of stimulation. The advice and assistance of Professors Paul F. Kerr and Ralph J. Holmes in regard to the mineralogical aspects of the study were genuinely appreciated.

To Dr. Harrison Schmitt I am indebted for assistance in the early stages of this investigation, when the guidance of an "old hand" at the leached outcrop problem was both needed and appreciated.

I should like to thank Professor Robert M. Garrels and Dr. Motoaki Sato for their discussion and advice regarding the preparation of Eh-pH diagrams in the section on boxwork structures.

Special help was rendered by Richard N. Hunt, Ralph Tuck, and Chauncey L. Thornburg, of the geologic staff, U. S. Smelting Refining & Mining Co. Warmest thanks are also due to the officials of the Peru Mining Co., especially to Joseph H. Taylor and Jerry W. Faust, for making the properties of that company available for study; to Edward B. Jennings, of the Universal Exploration Co., and the officials of the American Zinc Co. of Tennessee, for similar privileges on their properties; to Messrs. M. C. Haas, F. L. Wingfield, and W. H. Triplett, of the Cia. Minera de Pefioles, S.A., of Mexico, for like favors; to Mr. Russell Anderson, of the Utah Copper Co., for an informative tour of the Bingham Pit; to Robert B. Raup and Bernhard Felber, associates at various stages of this study; and to Karl Turekian, Paul Drummond, Hubert Barnes, and Paul Barton, former fellow students at Columbia University.

Mineralogy of Limonite in Lead-Zinc Gossans

GENERAL REMARKS

The term "limonite" is accepted today as referring to any natural aggregate of unidentified hydrous ferric oxides lacking apparent crystallization (Locke, 1926, p. 103). Posnjak and Merwin (1919) proved for the first time that goethite and lepidocrocite are the only valid members of what was formerly thought to be the "limonite series" of hydrates of ferric oxide. These two minerals have the same chemical composition ($Fe_2O_3 \cdot H_2O$) but differ in the nature of their hydrogen-oxygen bonding (Bragg, 1937, p. 111-113). In 1944, by chemical analysis of 20 gossan specimens, Blanchard demonstrated the variable composition of impure substances commonly grouped under the heading of limonite. To date, however, there has been no extensive study of variation in the occurrence of the two limonite minerals in lead-zinc gossans, mainly because of the difficulties involved in their identification by optical means.

When, in 1951, Kulp and Trites stated that goethite and lepidocrocite could be identified by differential thermal analysis, the identification of these minerals in many gossan samples seemed practicable for the first time. After an application of this technique to nearly 100 samples of natural hydrous ferric oxide, these writers concluded that:

> The thermal curves of goethite and lepidocrocite are sufficiently different to permit semi-quantitative estimation of these minerals in natural mixtures. The common occurrence of lepidocrocite in most aggregates of natural hydrous ferric oxide (limonite) is surprising.

The standard thermal analyses for goethite, lepidocrocite, and goethite-lepidocrocite mixtures are shown in Figure 1. These are typical curves from the original publication by Kulp and Trites.

The same writers suggested a possible application of their technique to hydrous ferric oxides in leached ore outcrops:

> Differential thermal analysis appears applicable to a systematic study of gossans, since both goethite and lepidocrocite may be estimated semi-quantitatively. Systematic variations in the hydrous iron oxide minerals with the position of an ore body or with the type of ore mineral present might be expected. Such variations would certainly reflect changing geochemical conditions.

Following this suggestion, the present writer applied differential thermal analysis to many samples of gossan limonite collected in the

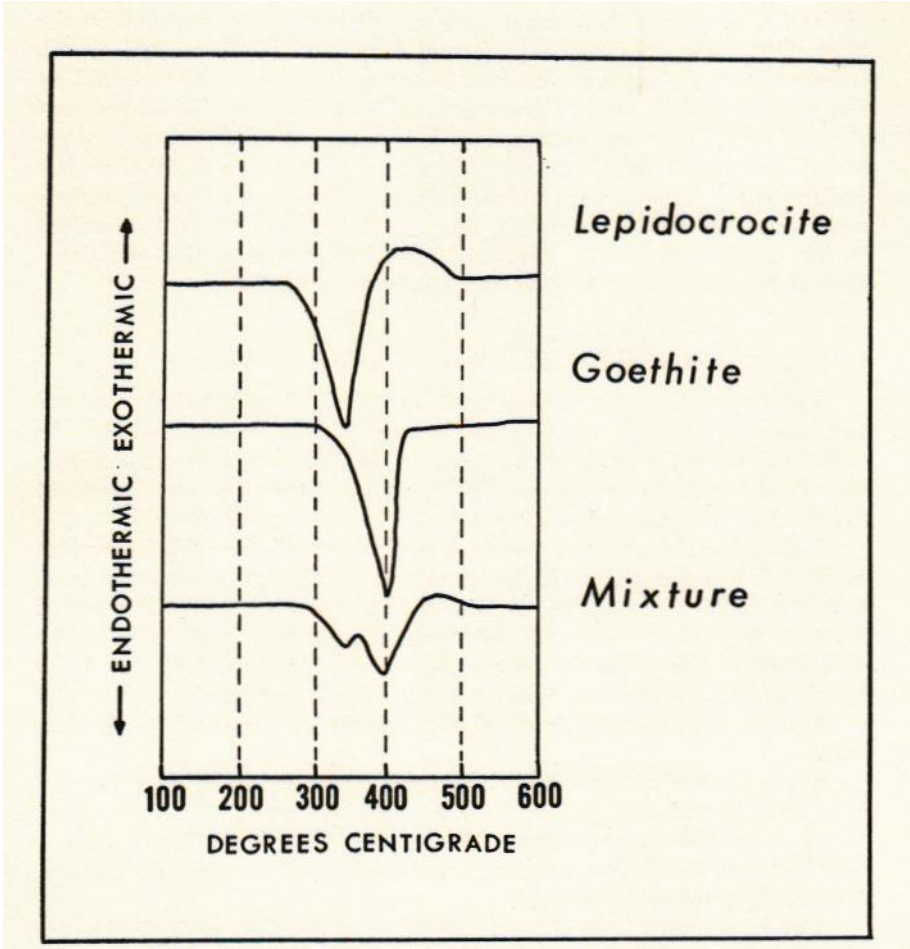

Figure 1

STANDARD DIFFERENTIAL THERMAL CURVES OF THE NATURAL HYDROUS FERRIC OXIDES

(After Kulp and Trites, 1951)

different mining localities where a close correlation between primary ore and leached outcrop could be established. Hydrous ferric oxides derived from very different primary sulfide sources were tested in the hope that variations in their thermal curves could be related to differences in their hypogene sources. Some specimens closely resembling the type limonites with "key structures" described by Blanchard and Boswell (1925-42) were analyzed to determine whether this technique would be useful in identifying limonites of similar derivation but lacking these recognizable features. In addition, a number of thermal analyses were made to detect any goethite-lepidocrocite variations which might aid in the distinction of indigenous and transported limonites as described by previous workers in this field.

EQUIPMENT AND PROCEDURE

The apparatus used in the thermal analysis of gossan limonites was the same equipment used by Kulp and Trites in establishing the standard curves for the hydrous ferric oxides. This equipment has been described by Kulp and Kerr (1949), and a theoretical treatment of differential thermal analysis is presented by Spiel et al. (1945).

A dual-terminal thermocouple is used to record the addition or loss of heat in the sample as its temperature is raised at a constant rate. One terminal of the couple is placed in the sample, and the other is inserted in a thermally inert substance (alundum). The temperature difference of this thermocouple is automatically plotted against oven temperature, and any heat change in the sample appears in the thermal curve as an endothermic or exothermic deviation from a straight base line.

Approximately 0.5 gram of limonite is consumed in a single thermal run, and if randomly picked from a hand specimen, this quantity of material provides a representative sample. This is confirmed by the constant reproducibility of thermal curves obtained for different samples from any given hand specimen.

The equipment is sensitive to amounts of goethite or lepidocrocite of over 10 percent in a mixture, and even lesser quantities may often be detected. All gossan samples were powdered (dry) at least to 200 mesh, to produce the greatest uniformity of grain size and therefore maximum peak sharpness. The thermal runs usually were continued to 600°C at a constant heating rate of 12°C per minute. At 600°C, the characteristic thermal reactions of the hydrous ferric oxides are complete, but some samples were heated to 1,000°C if the presence of impurities was suspected.

All told, 159 analyses were performed on gossan specimens, of which 47 were duplicates to check the reproducibility of the *curves*. Some of the original standard samples tested by Kulp and Trites were interspersed with gossan analyses to assure standard conditions.

RESULTS OF THERMAL ANALYSES OF GOSSAN LIMONITES

Thermal curves typical of those obtained from gossan limonites derived from different primary sources are presented in Figure 2, and the samples are described in Table 1. Comparisons of these curves with the standard thermal analyses for goethite and lepidocrocite left considerable doubt as to the true identity of the iron oxides present in the outcrop samples. The fact that no double endothermic peaks were obtained in any of the curves seemed, at least, to rule out the occurrence of goethite-lepidocrocite mixtures. Many of the curves, however, corresponded to standard lepidocrocite analyses, whereas others had the shape of goethite curves but with the endothermic reaction appearing at lepidocrocite temperatures.

X-ray powder patterns were obtained for 35 of the samples tested thermally; without exception, these proved to be goethite patterns. No lepidocrocite lines were seen in any of the X-ray films. The d-values and visual-line intensities for 25 of the 35 gossan limonites X-rayed are presented in Appendix E. Five reference patterns (samples 1 to 5) for goethite are also shown for comparison.

The goethite in these gossan samples was so poorly crystallized that it decomposed at temperatures well below the reaction of well-crystallized goethite samples tested by Kulp and Trites. This lowering of the reaction temperature of goethite is too great to be attributed to the small particle size of the sample or to the presence of impurities. In an early, unpublished paper, Trites (1948) described goethite specimens containing as much as 70 percent inert hematite, which decomposed at 411°C. When poorly crystallized gossan goethite was mixed with well-crystallized goethite and both were ground to a fairly uniform particle size (200-300 mesh), the resulting thermal curves (fig. 3) frequently matched standards for goethite-lepidocrocite mixtures. In these analyses, the lower temperature peaks represent decomposition of the poorly crystallized gossan goethite, and the peaks around 400°C, the decomposition of the coarsely crystalline goethite. The variable exothermic reactions in curves 2 and 3 of Figure 3 are due to a phase change of gamma to alpha Fe_2O_3. These reactions occurred within the gossan goethite portions of these samples and are here superposed on the mixture curves. They will be discussed below.

Viewed under the electron microscope, the gossan goethites (plate 1B) showed only slight evidences of crystallization even at very high magnifications, whereas all the standard goethites were very well crystallized (plate 1A).

Although the gossan limonites gave definite goethite X-ray powder patterns, the lines were broad, and in many films the known lines of lesser intensity were indistinct or missing. When tested on the X-ray diffractometer, the goethites used by Kulp and Trites in their work

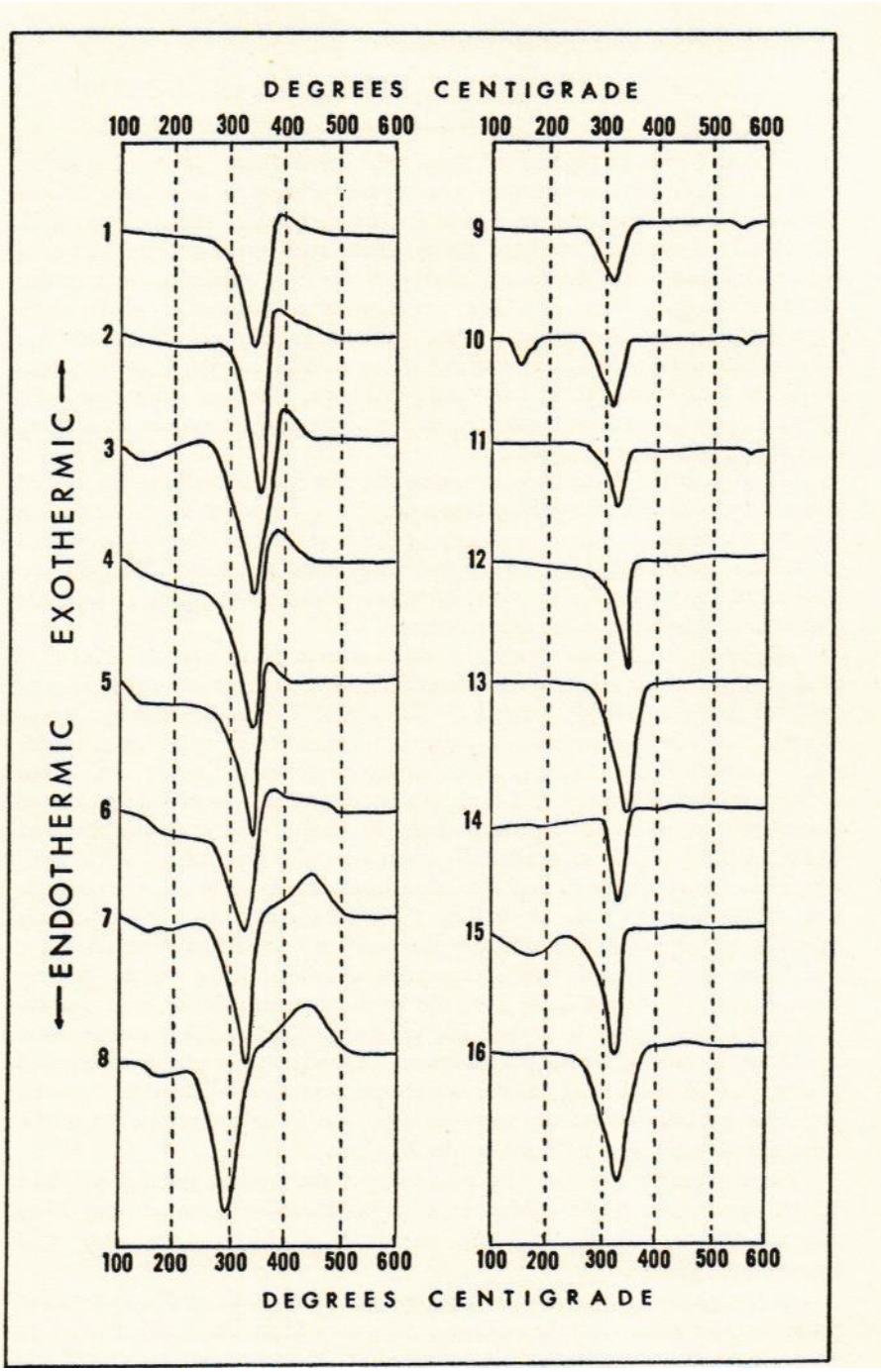

Figure 2

DIFFERENTIAL THERMAL CURVES (REPRESENTATIVE OF 112 ANALYSES)
OF GOSSAN LIMONITES

TABLE 1. GOSSAN LIMONITE SAMPLES TESTED BY THERMAL ANALYSIS

THERMAL CURVE	LOCALITY	DESCRIPTION
1	Providencia mine Zacatecas, Mexico	Limonite forming boxworks(?) after sphalerite. Primary ore: vertical chimneys of high-grade lead-zinc ore in limestone. Pyrite high in ore and locally dominant sulfide. Gangue: both carbonates and quartz.
2	Capote mine Sonora, Mexico	Indigenous limonite from gossan over cupriferous pyrite veins. Cubic voids. Sample picked from voids and adjacent areas.
3	Grant County mine Hanover, New Mexico	Limonite from pyrite gossan. Cubic voids. Gangue (thuringite) thoroughly altered to goethite. Original material: pyrite in chloritized shale.
4	Pewabic mine Hanover, New Mexico	Limonite from pyrite gossan. Original material: cubic pyrite in completely chloritized granodiorite dike. Gangue weathers to limonite at surface.
5	Grecian Bend ore body New Mayberry mine Bingham, Utah	Limonite from capping directly over auriferous pyrite replacement ores in quartzite.
6	Hobo vein Bullfrog mine Vanadium, New Mexico	Limonite from pyrite gossan. Cubic voids. Original material: pyrite disseminated in chloritized granodiorite.
7	Elizabeth mine Strafford, Vermont	Limonite from thin (2- to 5-ft) capping over pyrite-chalcopyrite-pyrrhotite ore in phlogopite-tremolite-carbonate rock.
8	Milan mine New Hampshire	Limonite in capping over pyrite-chalcopyrite lenses in schist. Gangue: chiefly quartz; some cordierite.
9	Anita mine New Mexico	Siliceous limonite forming ridges in boxwork after sphalerite. Original ore: about 4% Zn, 6% Pb, 0.5% Cu, low pyrite. Lead-zinc veins in basalt and granodiorite. Gangue chiefly quartz.
10	Bullfrog mine Vanadium, New Mexico	Siliceous limonite forming ridges in leached sphalerite cavities. Primary ore: 5%-25% Zn, 0.5%-1.0% Pb, low Cu. Pyrite low to moderate in ore. Gangue chiefly quartz and granodiorite fragments.
11	Grant County mine Hanover, New Mexico	Coatings of limonite and hematite in gossan voids after marmatite. Some siliceous impurities. Primary ore: marmatite in chloritized shale. Massive marmatite with little pyrite. No copper or lead.

TABLE 1. GOSSAN LIMONITE SAMPLES TESTED BY THERMAL ANALYSIS (continued)

THERMAL CURVE	LOCALITY	DESCRIPTION
12	Shingle Canyon mine New Mexico	Limonite from poorly developed sphalerite boxworks in siliceous gossan. Negligible pyrite and galena in primary ore. No copper. Gangue chiefly silica and kaolin.
13	Hidden Treasure mine Ophir Hill area Utah	Limonite forming ridges in well-formed boxworks after galena and sphalerite. Primary ore: galena dominant, low copper, low pyrite. Gangue chiefly carbonates.
14	New Mayberry mine Bingham, Utah	Limonite in capping over lead-replacement body in limestone. Much relict galena in outcrop. Primary ore: galena dominant, minor pyrite, no copper. Gangue chiefly quartz.
15	Pewabic mine Hanover, New Mexico	Limonite in cavities after sphalerite. Sample also contained limonite after gangue (salite). Primary ore: sphalerite in pyrometasomatic silicates (ilvaite, salite, hedenbergite). Minor pyrrhotite in ore.
16	Lark vein Bingham, Utah	Limonite forming boxworks after galena and sphalerite. Primary ore: lead-zinc veins in limestone and quartzite. Galena dominant, sphalerite, small quantities of pyrite and chalcopyrite. Gangue of quartz, clays, country-rock fragments.

gave sharp peaks high above background, whereas the gossan goethites gave broad, indistinct reflections.

Others have had difficulty in attempting to apply differential thermal analysis to identification of the natural hydrous ferric oxides. Studying goethite derivatives of hedenbergite, Federico and Fornaseri (1953) obtained curves which did not agree with the standards. As in the case of the gossan oxides, the goethite samples tested by them decomposed at 320°C, down in the standard lepidocrocite range.

These results were of mineralogic interest in showing that the standard differential thermal curves for goethite, for lepidocrocite, and for goethite-lepidocrocite mixtures can be produced by goethite alone, the variations depending upon the degree of crystallization in the materials analyzed. However, for the practical purposes of this gossan study, the results were negative in that they revealed no new outcrop guides of value in the search for ore.

The thermal curves of gossan limonites were surprisingly uniform and showed no variation with the grade, gangue, or country rocks of

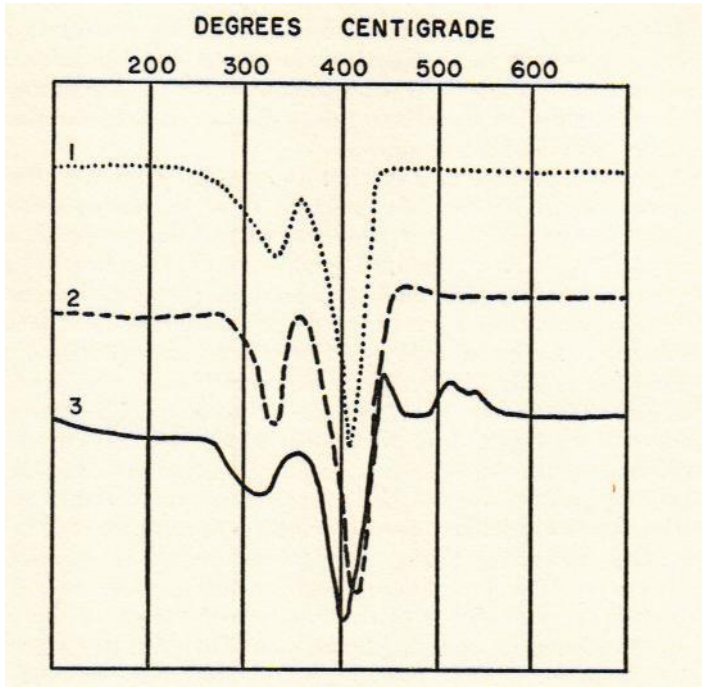

Figure 3

THERMAL CURVES OF GOETHITE MIXTURES

1. 50% well-crystallized goethite, from Restormed mine, Cornwall, England. 50% poorly crystallized goethite, from gossan of the Hidden Treasure mine, Utah.
2. 50% well-crystallized goethite, from Siegen, Prussia.
   50% poorly crystallized goethite, from gossan of the Pewabic mine, Hanover, New Mexico.
3. 50% well-crystallized goethite, from Friedrichsrode, Thuringia. 50% poorly crystallized goethite, from limonite pseudomorph after pyrite, Ashboro, North Carolina.

All mixtures were ground to pass a 200-mesh screen.

the original ores. The only primary feature that seemed to affect the limonite formed in the gossan was the relative abundance of original pyrite. Goethite after pyrite alone or after lead-zinc ores very high in pyrite produced thermal curves with marked exothermic reactions following the endothermic peaks (fig. 2, curves 1-8). Similar curves were obtained from goethite pseudomorphs (poorly crystallized) after pyrite. The exothermic peaks were not present in the thermal curves of goethite after lead-zinc ores of low to moderate pyrite content (fig. 2, curves 9-16).

The practical significance of these differences in the curves is limited; they merely appear where pyrite has been abundant but provide no

quantitative measure of that abundance. Furthermore, exothermic peaks also appeared in thermal curves of the few limonites of chalcopyrite and magnetite derivation that were tested; therefore, this reaction is not an exdusive indicator of pyrite as distinct from these other minerals in the primary iron source.

As yet, no satisfactory explanation can be given for the erratic appearance of the exothermic peaks in these gossan goethite curves. X-ray analyses of the heated products chilled at the peaks of endothermic decomposition produced gamma-Fe_20_3 (maghemite) patterns when an exothermic peak had appeared in the goethite curve, and alpha-Fe_20_3 (hematite) patterns when the exothermic peak was absent, indicating that the exothermic reaction was a phase change of gamma-to alpha-Fe_20_3. This phase change is usually associated with lepidocrocite, but these gossan limonites are all goethite. The conversion of gamma- to alpha-Fe_20_3 does not appear in the thermal curves of well-crystallized goethite, because it is very rapid above 400°C and the loss of heat is supposed to be too fast to register on the thermal apparatus. Since the poorly crystallized gossan goethites decompose well below this temperature, the phase change might be expected to appear in their thermal curves. The lower decomposition temperature would not explain, however, the absence of this reaction in curves of limonites derived from low-pyrite sources. Small amounts of water vapor might catalyze the phase change (Gheith, 1953), but those limonites which produced the exothermic reaction probably contained more uncombined water than those which did not. This is indicated by the low-temperature endothermic drift in curves 1 to 8, Figure 2. An additional feature, difficult to explain, is the fact that the exothermic reactions in some of the high-pyrite derivative curves continued well above 400°C, past the point where the phase change is supposed to be instantaneous.

A number of samples of limonite of a clearly transported origin were analyzed for comparison with indigenous oxides in each of several districts studied. The transported oxides were characterized by laminated, botryoidal, or stalactitic structures. Again, no differences were noted in the thermal curves which would be of practical aid in drawing the significant distinction between these two types of limonite. X-ray studies of transported limonites again showed the absence of lepidocrocite and the predominance of goethite.

PREDOMINANCE OF GOETHITE IN LEAD-ZINC GOSSANS

The predominance of goethite in lead-zinc gossan limonites is consistent with the experimental conditions under which the two limonite minerals were synthetically prepared in the laboratory (Goldsztaub, 1935; Weiser, 1935). Goethite is formed by the slow hydrolysis of most ferric salts (the chloride excepted) or by the aging of the gel

formed by the oxidation of ferrous compounds. On the other hand, lepidocrocite forms on oxidation of newly prepared hydrous FeS, $2Fe_20_3 \cdot 3Fe0$, Fe_2S_3, and hydrous Fe_30_4. It is also obtained on oxidation of ferrous chloride in the presence of sodium azide or pyridine under controlled pH conditions. It is apparent that the experimental conditions so far found favorable to the formation of goethite are more analogous to the natural conditions in the zone of oxidation. The known reagents used in the laboratory to form lepidocrocite would be absent, whereas the gels derived from ferrous compounds and solutions of ferric salts, especially the sulfate, would be common in the oxide zone.

In a study of the system Fe_20_3-SO_3-H_20, Posnjak and Merwin (1922) found that goethite is formed by hydrolysis of dilute ferric sulfate solutions at temperatures below 130°C. They obtained no lepidocrocite from this system, which is, at present, our best approximation to the natural environment for iron in the oxide zone.

POSSIBLE APPLICATION OF THERMAL ANALYSIS TO COPPER GOSSANS

Although the application of differential thermal analysis to lead-zinc gossan limonites brought out little in the way of new criteria for the prediction of hidden ores at depth, it would seem that an application of this technique to leached copper-ore outcrops might bring a greater return in practical results. Tunell (1930; see Locke, 1926, p. 105-107) has shown that the copper outcrops at Morenci, Bingham, and Tyrone contain hematite and jarosite as well as goethite, and that the ratios of these minerals are significant as guides to the type of original ore. Thermal analysis would provide a rapid means for an otherwise difficult determination of the proportions of these minerals in a gossan specimen. Standard curves for the analysis of the mineral ratios in natural aggregates could be set up with artificial mixtures of known proportions. Jarosite has a very distinctive thermal curve, with two prominent endothermic reactions at 460°C and 800°C (Kulp and Adler, 1950). Since it has been shown here that gossan limonites decompose at temperatures well below 400°C, probably owing to their poor crystallization, there should be little interference between the thermal peaks of goethite and jarosite. Hematite could be estimated from its depressive effects on the peak amplitudes of the two other minerals. This approach would be especially applicable to iron cappings over the porphyry-copper type of ore.

Interpretation of Boxwork Structures

GENERAL REMARKS

The most substantial contribution to our present knowledge of leached-ore outcrops has been, perhaps, the interpretation of the various limonite textures and structures derived from the common ore sulfides. It is to Roland Blanchard, P. F. Boswell, and Augustus Locke that we are indebted for the greater part of this research (1925-1942). The indigenous and transported limonite structures described by these writers were of immeasurable value in the identification and selection of samples for the analyses carried out in the present study. Many times, the only direct clue to the nature of the original sulfides in a leached outcrop was the presence of suggestive textures or structures in the residual limonite.

As a result of their proven significance as guides to primary mineralogy, indigenous boxwork structures are always sought in the examination of possible leached-ore outcrops. This emphasis placed on cellular sulfide derivatives may tend, however, to overshadow the fact that boxworks may also originate by differential leaching of nonsulfide structures. Locke recognized the occurrence of such nonsulfide boxworks and pointed out the confusion which may arise in the interpretation of "fine limonite sponges" and "fluffy limonite" replacing carbonate (1926, p. 134-137). These and other structures may be deceptively similar to indigenous sulfide derivatives, and so their recognition at the surface is a matter of practical importance. Nonsulfide boxworks were so commonly encountered during this investigation that they merit discussion here.

EXAMPLES OF NONSULFIDE BOXWORKS

COPPERSIDE MINE, GOODSPRINGS, NEVADA

The ore deposits of the Copperside mine have been described by D. F. Hewett (1931). In the brecciated dolomite below the copper stopes of this mine, an exposed mass of about 3 cubic yards of very coarse cellular limonitic jasper was found (P. B. Barton, Jr., personal communication, 1954). This mass was not surrounded by the usual halos of copper ore above. It is believed to have formed from solutions bearing iron and silica which moved downward into the brecciated ground below the sulfide ores, where limonitic jasper formed by filling and replacement along cracks in the shattered dolomite. Subsequent leaching of the dolomite brought out a coarse system of ridges and voids.

This structure, shown in Plate 2A, is strikingly similar to the coarse limonite boxwork that is usually correlated with mixtures of chalcopyrite and pyrite. The walls are thin, straight, and brittle. They

separate angular cavities ranging in size from 0.1 to 5.0 cm. The larger voids are not crossed by interstitial limonite structures. Locally, there are drusy coatings of white crystalline quartz, dolomite, and crustiform limonite along, but not within, the cell walls.

Without supplementary data, a hand specimen of this material could not be distinguished from true boxworks derived from pyritechalcopyrite ore.

NEW MAYBERRY MINE, UTAH

Limonite boxworks of similar origin but different appearance (pl. 2B) were found in the pyritic Grecian Bend ore body of the New Mayberry mine in Utah (Bingham district). Formed by the deposition of limonite in shattered limestone adjacent to the ore, these nonsulfide boxworks appear in the iron-stained country rock as cellular masses in which polygonal voids (0.2 to 4.0 cm across) are separated by dark-brown, slightly siliceous ridges. These ridges represent the original fracture network in the limestone and range in thickness from less than 0.1 mm to 2.0 mm. Along the middle of each ridge, the limonite is darker and more siliceous, whereas outward it becomes less siliceous and takes on a light yellow color. Some of the cavities are filled with limonite of the "fluffy" variety which, according to Blanchard (1939, p. 18-19), forms when ferric sulfate solutions attack a strong neutralizer like limestone. The presence of this type of precipitate in the voids provides one clue to the nature of the original material.

The randomness of the pattern of ridges and voids and the abundance of "fluffy" limonite which comprises the bulk of this structure serve to distinguish this boxwork from an indigenous sulfide derivative. The presence of some large cavities with little interstitial limonite suggests a wholesale removal of $CaCO_3$ rather than the leaching of iron-bearing sulfides. This, however, is not a reliable criterion, because some of the coarser sulfide derivatives have cavities free of interstitial fillings or structure.

HIDDEN TREASURE MINE, OPHIR HILL AREA, UTAH

A fine, cellular limonite most similar to products derived from galena was found in association with the ore outcrops at the Hidden Treasure mine in the Ophir Hill area, Utah. Iron-bearing solutions released on oxidation of the ores have penetrated the surrounding limestone country rock, causing precipitation of exotic limonite along fractures. Where this fracturing is intense, the pattern of limonite veinlets becomes complex and, after the leaching of the carbonates, emerges as an intricate system of ridges and voids (pl. 3A). This material shows a preferred direction of subparallel ridges, but filling and replacement along less systematic discontinuous cross-fractures has served to isolate small chambers of an angular to subrectangular shape. The limonite ridges display neither the delicacy nor the rigid parallelism of galena

derivatives, and lack the detailed structures of interstitial limonite associated with the finer boxworks of sphalerite after chalcopyrite. The little interstitial limonite that does occur is seen as fine laminae coating (and therefore parallel to) the cell walls (fig. 4). The cavities themselves are small and range in size from 1 to 6 mm.

Lamellar smithsonite from the same locality has been described by G. F. Loughlin (1919). He ascribes structures such as the layered growths of zinc carbonate shown in Plate 3B to a rhythmic replacement of limestone by zinc sulfate solutions. These solutions, derived from the oxidizing ore body, penetrated the limestone wall rocks along fractures, from which they then permeated and replaced the calcium carbonate. By a process analagous to the formation of liesegang diffusion bands, the Ca is replaced by Zn at various stages in the advance of the zinc sulfate front. Loughlin attributes the open spaces between the ridges of smithsonite to shrinkage attending the mole-per-mole replacement. Where fracturing in the original limestone was close and complex, the present smithsonite structure is correspondingly complex. The lamellar smithsonite was not seen in place by the writer but, along with the limonite boxworks after limestone, was found in abundance on the surface dumps at Ophir Hill.

It is possible that the limonite boxworks described above might originate through replacement of one of the more complicated and detailed smithsonite structures. However, there was no relict smithsonite with the iron oxides, and there is no reason to believe that the limonite boxwork could not have formed by simple movement of iron solutions along a detailed fracture network in the limestone without an intermediate smithsonite stage.

Regardless of whether such limonite boxworks represent replacements of smithsonite or direct fillings and replacements in limestone, they might prove a source of confusion to an observer not aware of the fact that such structures may be of an entirely different origin from true sulfide boxworks.

LARK VEIN, BINGHAM DISTRICT, UTAH

Spongelike masses of hypogene silica were found along the leached outcrops of the Lark vein in Utah (appendix A). The quartzite adjacent to this lead-zinc vein is highly shattered and has been indurated in places by both hypogene and supergene silica. Locally, the quartzite is infiltrated by a system of very fine hypogene quartz veinlets from 0.1 to 1.0 mm wide. Under the microscope, these are seen as dense symmetrical vein fillings of microcrystalline quartz. The quartz is elongated normal to the walls and shows a radial or comb structure with wavy extinction. The boundaries of the veinlets are sharp.

Exposed to weathering, the silica veinlets prove more resistant than the quartzite host. The latter is etched out, forming siliceous boxworks in which the cavities and ridges are very irregular and reflect the random

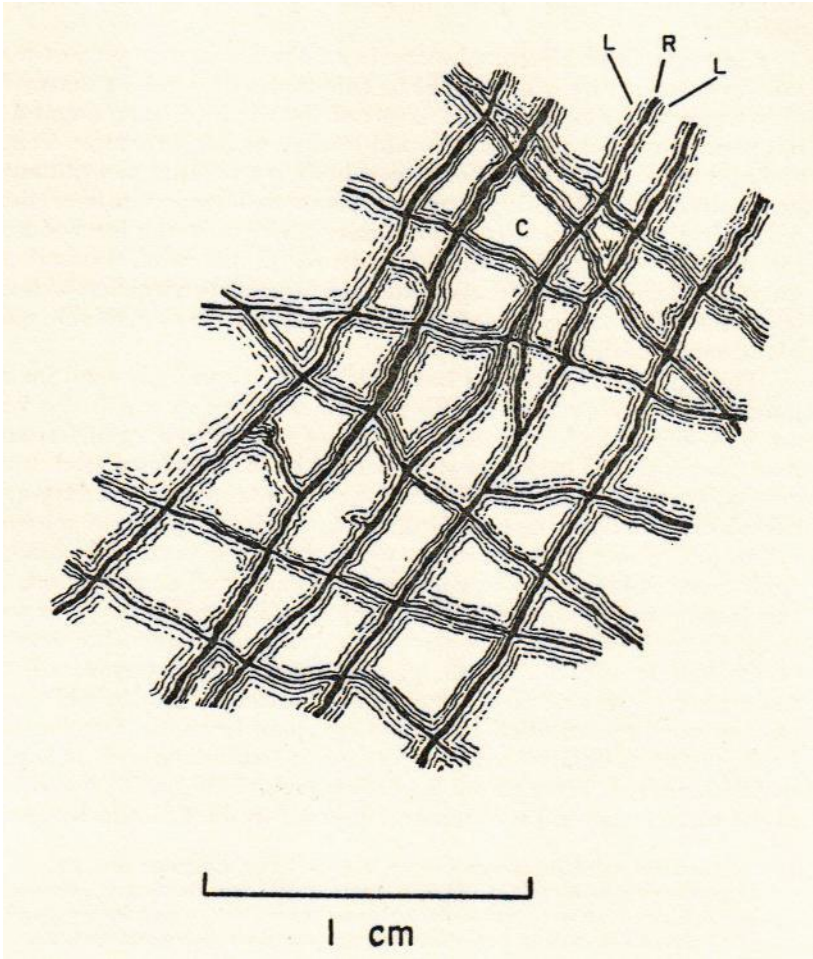

Figure 4

BOXWORK AFTER LIMESTONE, HIDDEN TREASURE MINE, UTAH

Diagrammatic sketch of structure seen in Plate 3A. A subrectangular system of ridges (r) of dark-brown limonite is shown. The small cavities (c) are coated with fine, light-yellow laminae (1) of limonite. The fact that yellow coatings parallel the cell walls distinguishes this boxwork from similar sulfide derivatives. Interstitial limonite in true sulfide boxworks generally projects into the cavities as unconnected ridges and rosettes. Scale X 3.

pattern of the original system of silica veinlets within the fractured quartzite.

Although these siliceous boxworks of the Lark vein present a detailed void structure which might be confused with a sulfide derivative, they are confined to the surface layers of the silicified quartzite and do not penetrate the rock mass, as would leached sulfide structures. Veinlet and host materials do not differ greatly in their resistance to weathering; hence differential leaching is not sufficient to form extensive cellular masses in the outcrop. If closely examined, ridges in the leached areas can be traced directly into silica veinlets within the solid, unweathered quartzite. Residual fragments of unleached quartzite may even be found in some of the cavities (see pl. 4A), and these offer a dependable guide to the nature of the leached matter.

The expression "siliceous boxwork" is often carelessly used for any porous structure associated with leached outcrops in which the voids are well defined and separated by ridges of silica. From a genetic standpoint, boxworks of hypogene silica should be distinguished from super-gene siliceous boxworks formed during the oxidation process. Hypogene silica may penetrate fractured sulfides as a primary phase of mineralization and give rise to boxworks when the ore is eventually leached. Both types of siliceous boxworks may preserve sulfide structures, but this is more to be expected with supergene silica or jasper, which tends to infiltrate the sulfides along parting and cleavage planes characteristic of the sulfide mineral. In the writer's experience, hypogene silica is more generally found along fractures in shattered sulfides, which may or may not be controlled by crystallographic features. The fact that hypogene silica boxworks may form after nonsulfide as well as leached sulfide matter, is brought out by Callaghan's (1938, p. 33) description of the surface expression of mineral deposits in the Cascade Range:

> Leached sulphide ore commonly has a cellular structure, and an outcrop of quartz with cavities and thin filaments indicates the former presence of sulphides. However, quartz that contained carbonate, or angular lumps of clay minerals or sericite has a similar appearance on weathered surfaces.

Callaghan recalled that these quartz filaments are commonly stained with iron oxide, but that some are almost *pure* white (personal communication, November 1956).

BOXWORK SIDERITE

Boxworks of siderite have long been known as examples of cellular, nonsulfide structures (pl. 4B) and were first reported at Bisbee, Arizona. Formed by the precipitation of supergene siderite in limestone below the iron-copper sulfide ore bodies, they serve as underground guides to overlying ore in that district. As indicated by Trischka et al. (1929), this siderite may alter to limonite, which then inherits the boxwork form. The limonite structure is usually less competent and is "crushed and

compressed by the weight of overlying rocks." If, however, such boxworks of siderite, or of its limonite alteration product, were preserved and exposed at the surface, they would indicate the removal of overlying ore by erosion rather than the possible existence of ore beneath the outcrop.

It is questionable whether boxwork siderite would have the same meaning in every district where it might be found. The late Paul G. Leroy (personal communication, September 1954), recently engaged in a study of the disseminated copper ores at Santa Rita, described an interesting underground occurrence of siderite in that district:

> Boxworks of siderite occur in many places at the Oswaldo No. 2 Mine, Santa Rita, New Mexico. Where best developed, such boxwork consists of rhombohedral chambers up to 1/2 cm. in largest dimension, with walls of finely crystalline, light-buff to greenish siderite. Pyrite, though sparse, can sometimes be seen encased in the siderite.
>
> Chemically, the siderite is not pure $FeCO_3$ but rather contains substantial amounts of magnesium. It contains no zinc.
>
> The siderite boxwork may be well developed for a distance of several ***feet*** along the walls of a drift (e.g., along W428). The rock in which the boxwork is found is the Hanover limestone.

The enclosure of pyrite and the absence of zinc in this boxwork material suggests that the siderite may have been hypogene. The supergene boxworks at Bisbee contained over 5 percent zinc, showing that siderite which forms from solutions draining from an oxidizing ore body can be expected to contain considerable amounts of the soluble metals, other than iron, which may have been present in the primary ore. At the Oswaldo mine, however, the siderite boxwork was associated with the zinc ore bodies and still "contained no zinc."

Unlike boxworks of supergene origin, which depend on solutions derived from oxidizing ore for their formation, hypogene siderite should not be expected to bear any definite spacial relationship to ore. In general, there would be no reason to expect localization of hypogene siderite in the ground below an ore body.

The differences between hypogene and supergene siderite may warrant additional study in view of the significance that can be attached to one and not the other. Hypogene characteristics such as those shown by the boxwork siderite at Santa Rita (i.e., the absence of copper or zinc, the encasement of pyrite, and *perhaps* the presence of substantial amounts of $MgCO_3$) might aid in making the correct interpretation.

A CASE HISTORY IN BOXWORK INTERPRETATION

In the earlier stages of this investigation, difficulties in the interpretation of commonly occurring nonsulfide boxworks were attributed to the author's lack of experience. As the study progressed, however, it was soon realized that others whose work involves frequent examination

of ore prospects often have similar difficulties in distinguishing between nonsulfide void structures and boxworks after the ore minerals.

An actual case of this sort is presented by the outcrops at Calera, Chihuahua, Mexico. Here, surface exposures of coarse siliceous box-works seemed to offer promise of sulfides underground and encouraged officials of the Compania Minera de Perioles to drill on their property. Special care was taken to avoid missing the favorable structure at depth, but the drilling revealed no sulfide ore body beneath the surface.

D. F. Dill (unpublished company report, April 8, 1953) reported that:

> Our expectations of finding primary sphalerite below the surface exposure of the silicified material and favorable looking boxwork was not substantiated by the drilling. Only in holes 1 and 4, in line with the concentration of heaviest boxwork, was the silicified zone intersected, and here it showed decreasing width, six meters at 40 meters depth down to three meters at 100 meters depth. In both holes, the proportion of cellular cavities to total volume of silica was small, and there were no traces of sulfides in the cavities. We still do not know what mineral formerly occupied the cavities in the boxwork and can only guess that it might have been calcite, recrystallized limestone, or hematite, but probably not sphalerite.

The boxwork considered here (pl. 5A) consists of silica, white when fresh but tan to black on exposed surfaces that are coated with iron and manganese oxides. The ridges vary in thickness from 0.2 to 2.0 mm and separate cavities 0.5 to 10.0 mm in width. For the most part, the cell walls are well connected but discontinuous. In places, they are sufficiently intricate to give an impression of delicate structures along cleavage and parting planes in former sulfides.

Several facts strongly suggest that the original interpretation of the boxworks at Calera was correct; namely, that they *are* true sulfide derivatives. The abundance of iron oxides coating the boxwork implies that the leached material was iron bearing, and renders the idea of an original sulfide more tenable than leached calcite or recrystallized limestone. It is possible that the leached material was hematite, but there is no reason to believe that hematite would undergo such extensive leaching. Furthermore, the form of boxwork is not at all suggestive of original hematite.

The strongest evidence in favor of sphalerite as the original material is the presence of strong residual zinc traces in the boxworks at the surface. Although no signs of relict zinc minerals were evident under the microscope, simple microchemical tests revealed that there was still a considerable trace of zinc. X-ray fluorescence tests showed that *even* the white quartz in the ridges (free of limonite) contained zinc. The actual quantity of this trace was determined by dithiozone analysis as 0.19± .002% zinc by weight.[1] The coatings in the cells re-

[1]The writer is indebted to Hubert L. Barnes, who was kind enough to determine the amount of zinc in this sample. He employed a dithiozone method adapted from that of Almond and Sandell (1951).

sponded positively to the potassium mercuric thiocyanate test for zinc described by Short (1940, p. 187-190).

The specimen to the right of the Calera boxwork in Plate 5A shows a system of hypogene silica veinlets in iron-rich sphalerite which are identical in scale and pattern to the system of silica ridges in the Calera boxwork. Isolated veinlets locally cut across the specimen for distances up to several centimeters before linking with other veinlets or branching into a detailed angular network of veinlets which shows no apparent control by crystallographic directions in the fractured sphalerite. If such a specimen were oxidized and leached, the zinc would tend to depart, leaving behind an iron-stained boxwork almost identical to that which caused the confusion at Calera.

The fact that sphalerite was not found at depth on the favorable structure at Calera does not mean that the surface boxworks were not derivatives of sphalerite, but that the ore body was shallow and that the portion which escaped erosion was oxidized and thoroughly leached. This merely emphasizes the point stressed by earlier workers in this field; that the discovery of favorable signs in gossan is no *guarantee* of ore at depth.

The case history at Calera is cited to illustrate the difficulties which may arise in the interpretation of a boxwork which does not have the definite earmarks of a sulfide derivative. The original interpretation in this area was that the cellular structure was inherited from an ore mineral. This decision was reversed when the drilling data came in, and now the writer proposes, on the basis of laboratory study of the boxwork, that the original interpretation was actually the correct one.

CHEMISTRY OF FORMATION OF SUPERGENE LIMONITE AND SIDERITE BOXWORKS AFTER LIMESTONE

PROBLEMS INVOLVED

The formation of a limonite or siderite boxwork after limestone requires (1) deposition of ferrous carbonate or ferric hydroxide along fractures in the country rock, and (2) subsequent or possibly simultaneous leaching of the calcium carbonate matrix. The exact chemical conditions which favor siderite as opposed to limonite, and which permit leaching of the carbonate matrix while the iron precipitates are preserved, have been a matter of some speculation in the past. Locke, writing in 1926, summarized his views on this subject as follows:

> Ferrous sulphate encountering limestone may make siderite. Whether in a given case to expect siderite, or "limonite," or a cave in limestone is difficult to decide, but at times it seems to us that the siderite bodies are produced mostly in saturated and the "limonite" bodies in aerated material. In some cases . . . the presence of copper would make the difference between siderite and "limonite."

In their discussion of the chemistry of formation of siderite boxworks after limestone at Bisbee, Trischka et al. (1929) pointed out some of the problems involved. As did Locke, they considered the oxidizing effect of cupric ion in the solutions from which the iron minerals might form, and questioned whether the precipitation of limonite rather than siderite might not signify the presence of copper in the nearby ore. They also discussed the predominance of ferrous or ferric ions in the solutions and postulated a pronounced change from ferric to ferrous solutions at the time that siderite is deposited:

> It has been shown that while ferrous sulphate reacting with limestone will yield siderite (ferrous carbonate), the ferric sulphate yields ferric hydroxide. To form siderite, then, there must have been a marked change in the solutions, which were relatively rich in ferric sulphate during oxidation of the sulphides and became low in ferric and rich in ferrous sulphate during formation of the siderite.

In spite of this reasoning, there does not seem to be a need for a "marked change in the solutions" which may never be high in ferric ion under the usual conditions prevailing in and below the oxide zone. An important role is always assigned to ferric sulfate as an oxidizing agent; yet, in the acid environment of the oxide zone, it is unlikely that the ferric ion would be nearly as abundant as the ferrous. The ferric ion may form if the acidity of the ferrous solutions is reduced by dilution, or by reaction with gangue, country rock, or more alkaline ground water. As soon as it forms, however, it is hydrolyzed and immediately thrown down as ferric hydroxide, leaving the solutions less rich in iron but still predominantly ferrous.

These and other problems are involved in the formation of supergene limonite and siderite boxworks after limestone.

DEPOSITION OF LIMONITE OR SIDERITE

The question of whether limonite or siderite will form in limestone below oxidizing ore can best be discussed in terms of the acidity and oxidation potential of the environment? An Eh-pH diagram for the system Fe-H_2O-CO_2-S has been prepared for this purpose and is shown in Figure 5. Deltombe and Pourbaix (1954b) had previously studied the iron-water-carbon dioxide system, and many of their equations were used in the construction of the upper parts of this diagram. The diagram of Krumbein and Garrels (1952), showing the stability fields

2. Since the present manuscript was submitted, Eh-pH diagrams of a different nature *have* been published for this same system. In an excellent study of the separation of manganese from iron in sedimentary processes, K. B. Krauskopf (1957) presents diagrams showing plots of many field boundaries over the entire range of natural acidities and oxidation potentials. As pointed out by Krauskopf, such diagrams do not define completely the stability fields of solids at equilibrium, but show the location of certain field boundaries for different acidities, oxidation potentials, and assumed ionic activities. They show very well the metastable precipitates that can be expected under different assumed environments.

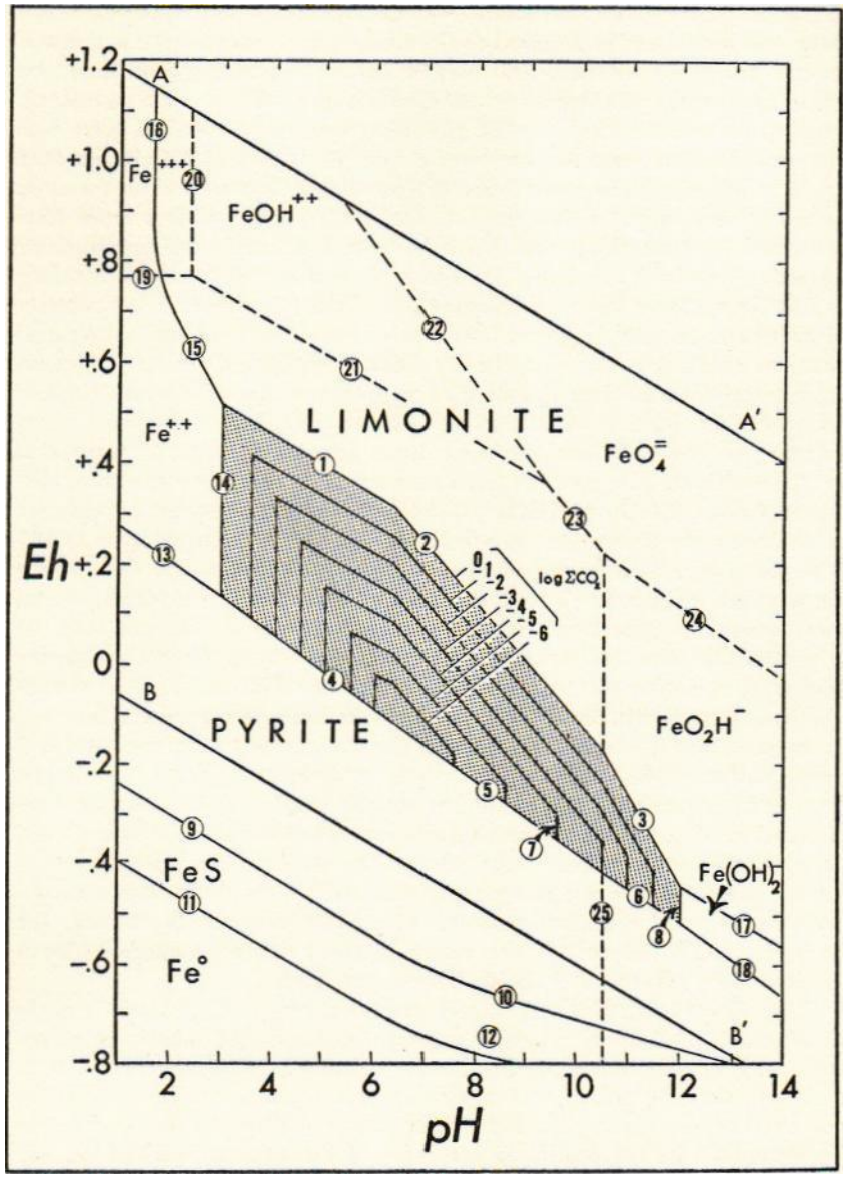

Figure 5

EH-PH DIAGRAM FOR THE SYSTEM FE-H2O-CO2-S IN THE OXIDE ZONE

The total dissolved sulfur is assumed to be 10^{-1} mole per liter. The stability field for siderite (stippled) is shown for concentrations of total dissolved CO_2 of from 10^{0} to 10^{-6} mole per liter.

of pyrite, siderite, and hematite, was derived for a sea water environment and could not be applied to the oxide zone, where there is a much greater range in acidity, and where different assumptions must be made as to total dissolved carbon dioxide and sulfur. The technique applied in constructing the Eh-pH diagram for the oxide zone was identical to that used by Deltombe and Pourbaix (1954a,b) in that equilibrium equations were derived from thermodynamic data for each stability boundary; in this respect, the methodology differs from that described by Krumbein and Garrels. The reactions and equilibrium formulae involved are listed in Table 2, and numbers corresponding to this listing have been placed on each of the equilibrium boundaries in Figure 5. In the diagram, boundaries between ions and solids and between solids are shown as heavy lines. Superposed on the diagram are a number of broken lines which represent the equilibrium boundaries between ions. A brief account of the procedure followed in calculating the equilibrium formulae from free-energy data is presented in Appendix B. The siderite field (shaded) is sensitive to the total dissolved CO_2 (H_2CO_3 + HCO_3— + CO_3^{--}) in the system; so siderite fields have been shown for total CO_2 concentrations of from 10^{-6} to 10° mole per liter. This range of assumed values would more than cover the natural variation to be expected in going from ore oxidizing in an inert quartz gangue and quartzite country rock, at one extreme, to saturated solutions in limestone, at the other. The change in the siderite field with variation of total dissolved carbon dioxide can best be visualized in Figure 6, where the field is shown in isometric perspective.

Figures 5 and 6 are based also on the assumption that the total dissolved sulfur (H_2S + HS^- + S^{--} + S_2^{--} + SO_4^{--}) is 10^{-1} mole per liter, or near saturation. This figure may approximate the composition of solutions descending from oxidizing ore into limestone. These would be predominantly sulfate solutions. The equilibrium boundaries in the Eh-pH diagrams are not greatly affected by making other assumptions as to total dissolved sulfur. The pyrite-siderite boundary, for example, shifts .02 volt if the assumed total sulfur is changed by a factor of 1,000 from 10—i to 10^{-4} mole per liter.

The Eh-pH calculations offer theoretical support to Locke's early observation that siderite bodies seem to be produced mostly in saturated, and the "limonite" bodies in aerated, material. From Figure 5, it is evident that the precipitation of siderite is favored by a low oxidation potential at any given pH. The greater the aeration of the ground, the higher would be the oxidizing intensity of the system, and the greater the likelihood of finding limonite as the stable precipitate. At a fixed pH, the critical Eh value marking the borderline between limonite and siderite predominance is controlled largely by the quantity of dissolved carbon dioxide in the system. Acid solutions saturated in CO_2 (ca. 10^{-1} mole/liter) which might be generated by oxidizing ore in limestone could theoretically form siderite at oxidation potentials as high

TABLE 2. REACTIONS AND EQUILIBRIUM FORMULAE FOR THE SYSTEM Fe-H_2O-CO_2-S IN THE OXIDE ZONE

1. SIDERITE-LIMONITE ($pH < 6.4$)
$$3H_2O + FeCO_3 = Fe(OH)_3 + H_2CO_3 + H^+ + 1e^-$$
$$E = .699 - .059\ pH + .059\ \log A_{H_2CO_3}$$
2. SIDERITE-LIMONITE ($6.4 < pH < 10.5$)
$$3H_2O + FeCO_3 = Fe(OH)_3 + HCO_3^- + 2H^+ + 1e^-$$
$$E = 1.076 - .118\ pH + .059\ \log A_{HCO_3^-}$$
3. SIDERITE-LIMONITE ($pH > 10.5$)
$$3H_2O + FeCO_3 = Fe(OH)_3 + CO_3^{--} + 3H^+ + 1e^-$$
$$E = 1.687 - .177\ pH + .059\ \log A_{CO_3^{--}}$$
4. PYRITE-SIDERITE ($pH < 6.4$)
$$8H_2O + H_2CO_3 + FeS_2 = FeCO_3 + 2SO_4^{--} + 18H^+ + 14e^-$$
$$E = .392 + .008\ \log A_{SO_4^{--}} - .076\ pH - .004\ \log A_{H_2CO_3}$$
5. PYRITE-SIDERITE ($6.4 < pH < 10.5$)
$$8H_2O + HCO_3^- + FeS_2 = FeCO_3 + 2SO_4^{--} + 17H^+ + 14e^-$$
$$E = .365 + .008\ \log A_{SO_4^{--}} - .072\ pH - .004\ \log A_{HCO_3^-}$$
6. PYRITE-SIDERITE ($pH > 10.5$)
$$8H_2O + CO_3^{--} + FeS_2 = FeCO_3 + 2SO_4^{--} + 16H^+ + 14e^-$$
$$E = .323 + .008\ \log A_{SO_4^{--}} - .068\ pH - .004\ \log A_{CO_3^{--}}$$
7. SIDERITE-FERROUS HYDROXIDE ($6.4 < pH < 10.5$)
$$2H_2O + FeCO_3 = Fe(OH)_2 + HCO_3^- + H^+$$
$$\log A_{HCO_3^-} = -13.62 + pH$$
8. SIDERITE-FERROUS HYDROXIDE ($pH > 10.5$)
$$2H_2O + FeCO_3 = Fe(OH)_2 + CO_3^{--} + 2H^+$$
$$\log A_{CO_3^{--}} = 23.95 + 2\ pH$$
9. PYRRHOTITE-PYRITE ($pH < 7$)
$$S^{--} + FeS = FeS_2 + 2e^-$$
$$E = -.837 - .030\ \log A_{S^{--}}$$
but $A_{S^{--}} = A_{H_2S} \cdot 10^{-21}/A^2_{H^+}$
$$E = -.217 - .030\ \log A_{H_2S} - .059\ pH$$
10. PYRRHOTITE-PYRITE ($pH > 7$)
$$S^{--} + FeS = FeS_2 + 2e^-$$
$$E = -.837 - .030\ \log A_{S^{--}}$$
but $A_{S^{--}} = A_{HS^-} \cdot 10^{-14}/A_{H^+}$
$$E = -.424 - .030\ \log A_{HS^-} - .030\ pH$$
11. NATIVE IRON-PYRRHOTITE ($pH < 7$)
$$S^{--} + Fe^0 = FeS + 2e^-$$
$$E = -.983 - .030\ \log A_{S^{--}}$$
but $A_{S^{--}} = A_{H_2S} \cdot 10^{-21}/A^2_{H^+}$
$$E = -.363 - .030\ \log A_{H_2S} - .059\ pH$$
12. NATIVE IRON-PYRRHOTITE
$$S^{--} + Fe^0 = FeS + 2e^-$$
$$E = -.983 - .030\ \log A_{S^{--}}$$
but $A_{S^{--}} = A_{HS^-} \cdot 10^{-14}/A_{H^+}$
$$E = -.570 + .030\ \log A_{HS^-} - .030\ pH$$

13. PYRITE-FERROUS ION

$$8H_2O + FeS_2 = Fe^{++} + 2SO_4^{--} + 16H^+ + 14e^-$$

$$E = .367 + .004 \log A_{Fe^{++}} + .008 \log A_{SO_4^{--}} - .067\ pH$$

14. SIDERITE-FERROUS ION

$$2H^+ + FeCO_3 = H_2CO_3 + Fe^{++}$$

$$\log A_{Fe^{++}} = 6.046 - 2\ pH - \log A_{H_2CO_3}$$

15. FERROUS ION-LIMONITE

$$3H_2O + Fe^{++} = Fe(OH)_3 + 3H^+ + 1e^-$$

$$E = 1.057 - .177\ pH - .059 \log A_{Fe^{++}}$$

16. FERRIC ION-LIMONITE

$$3H_2O + Fe^{+++} = Fe(OH)_3 + 3H^+$$

$$\log A_{Fe^{+++}} = 4.842 - 3\ pH$$

17. FERROUS HYDROXIDE-LIMONITE

$$H_2O + Fe(OH)_2 = Fe(OH)_3 + H^+ + 1e^-$$

$$E = .272 - .059\ pH$$

18. PYRITE-FERROUS HYDROXIDE

$$10H_2O + FeS_2 = Fe(OH)_2 + 2SO_4^{--} + 18H^+ + 14e^-$$

$$E = .422 + .008 \log A_{SO_4^{--}} - .075\ pH$$

19. FERROUS ION-FERRIC ION

$$Fe^{++} = Fe^{+++} + 1e^-$$

$$E = .771 + .059 \log A_{Fe^{+++}} - .059 \log A_{Fe^{++}}$$

20. Fe^{+++}-$FeOH^{++}$

$$H_2O + Fe^{+++} = FeOH^{++} + H^+$$

$$\log(A_{Fe^{+++}}/A_{FeOH^{++}}) = 2.430 - pH$$

21. Fe^{++}-$FeOH^{++}$

$$H_2O + Fe^{++} = FeOH^{++} + H^+ + 1e^-$$

$$E = .914 - .059\ pH - .059 \log(A_{Fe^{++}}/A_{FeOH^{++}})$$

22. $FeOH^{++}$-FeO_4^{--}

$$3H_2O + FeOH^{++} = FeO_4^{--} + 8H^+ + 4e^-$$

$$E = 1.652 - .138\ pH - .020 \log(A_{FeOH^{++}}/A_{FeO_4^{--}})$$

23. Fe^{++}-FeO_4^{--}

$$4H_2O + Fe^{++} = FeO_4^{--} + 8H^+ + 4e^-$$

$$E = 1.468 - .118\ pH - .012 \log(A_{Fe^{++}}/A_{FeO_4^{--}})$$

24. FeO_2H^--FeO_4^{--}

$$2H_2O + FeO_2H^- = FeO_4^{--} + 5H^+ + 4e^-$$

$$E = 1.001 - .074\ pH - .015 \log(A_{FeO_2H^-}/A_{FeO_4^{--}})$$

25. Fe^{++}-FeO_2H^-

$$2H_2O + Fe^{++} = FeO_2H^- + 3H^+$$

$$\log(A_{Fe^{++}}/A_{FeO_2H^-}) = 31.580 - 3\ pH$$

A-A′. $H_2O = \frac{1}{2}O_2 + 2H^+ + 2e^-$

$$E = 1.23 - .059\ pH$$

B-B′. $H_2 = 2H^+ + 2e^-$

$$E = 0.00 - .059\ pH$$

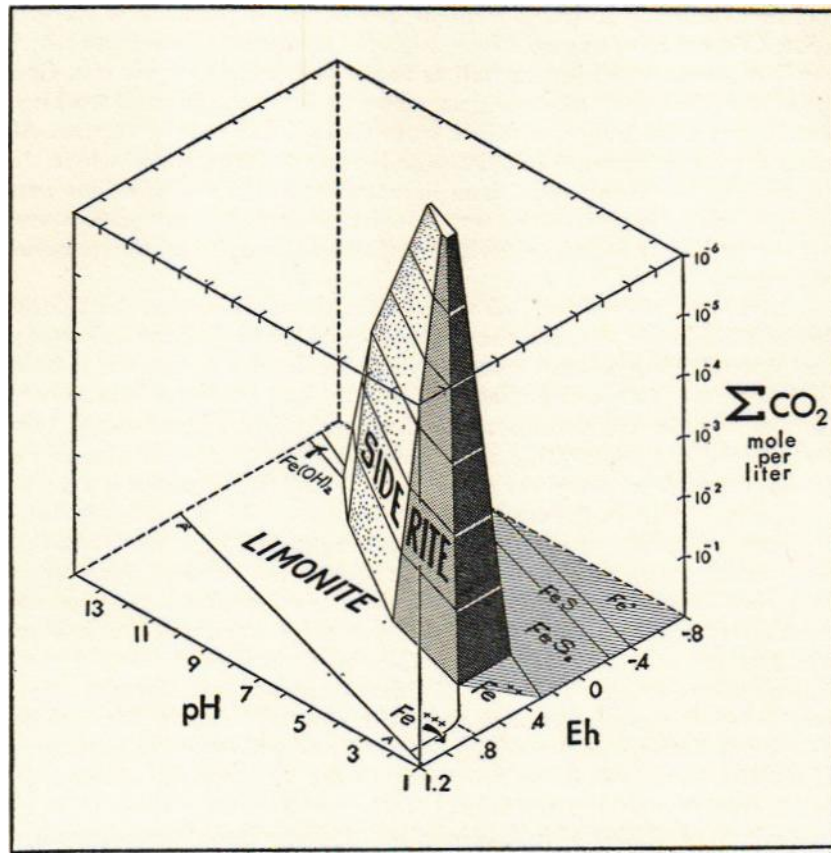

Figure 6

VARIATION OF THE SIDERITE STABILITY FIELD WITH DISSOLVED-CO2 CONCENTRATION

as + 0.4 volt, and this leads to the belief that the ferrous carbonate might form above the water table as well as below. Depletion of oxygen by the altering ore would assure the formation of siderite rather than limonite if the descending solutions even approached saturation in dissolved carbon dioxide.

The presence of cupric ions would certainly increase the oxidation potential of a system and would thereby promote the deposition of limonite. It might even be the deciding factor in borderline cases where a system was close to the Eh-pH boundary between siderite and limonite. However, if a body of limonite is intersected in exploratory underground workings, there is no way of evaluating the role of copper. The

fact that the body is limonite might be due to the presence of oxygen, a low CO_2 content, or a relatively high pH in the solutions from which the limonite formed, just as well as to the presence of cupric ion. Conversely, a discovery of supergene siderite in underground workings should not discourage the miner from thoughts of nearby copper. All other factors being constant, limonite is more to be expected where the cupric ion has accompanied iron in solution; but if the solutions were charged with dissolved CO_2, were low in pH, and did not have a very high oxidizing intensity, siderite would form in spite of the presence of copper.

As the quantity of total dissolved CO_2 becomes smaller, the siderite field diminishes in size, and the probability of forming limonite becomes correspondingly greater. Figure 6 illustrates, however, that the siderite field persists at CO_2 concentrations as low as 10^{-8} mole per liter. Therefore, with only slight amounts of dissolved CO_2, siderite might even form below the water table in a country rock such as quartzite, if the pH of the system were on the order of 6 to 7 and the Eh about —0.1 volt.

It is apparent in Figure 5 that the stability field of the ferric ion is restricted to a zone of very high oxidation potential (greater than 0.77 volt) and low pH (less than 2.5). The ferrous ion predominates under most conditions to be expected in the oxide zone, and it is the predominant ion in equilibrium with both ferrous carbonate and *ferric* hydroxide. During oxidation of sulfides, the solutions should contain more ferrous than ferric ion, because of the acids generated. These solutions may leave the ore body and enter the country rock to form either siderite or limonite, depending on the Eh and pH of the environment. If siderite is formed, it is due merely to the fact that the Eh and pH are favorable and the solubility product of ferrous carbonate is exceeded; no oxidation of iron is involved. If limonite is formed, the iron in solution must be oxidized, but hydrolysis of the ferric ion is so rapid that the solutions do not become predominantly ferric at any stage. The solutions are predominantly ferrous in the oxidizing ore and predominantly ferrous at the site of siderite *or* limonite deposition.

Another factor affecting limonite or siderite deposition is the temperature in the ground through which the solutions pass. The Eh-pH diagram is calculated for 25°C, but it is known that temperatures in the oxide zone range up to 50°C. Higher temperatures would favor the deposition of limonite by reducing the solubility of carbon dioxide in the descending solutions. Heat would have the general effect of reducing the size of the siderite stability field.

LEACHING OF THE CARBONATE MATRIX

Formation of the boxwork structure after deposition of limonite or siderite requires such chemical conditions that calcium carbonate is selectively leached while the iron precipitates along fractures are preserved. An attempt to define these conditions in quantitative terms of

one or two variables such as Eh or pH would be an oversimplification of the actual process in nature.

The leaching effect of descending solutions would be affected by variations in temperatures, acidity, oxidation potential, CO_2 concentration, and the relative solubility and rates of solution of siderite, limonite, and calcite. In general, it might be postulated that the formation of a cave in limestone below ore indicates leaching by solutions so highly acid that both calcite and the iron minerals are soluble, and that the formation of a siderite or limonite boxwork is indicative of a milder acidity favorable to solution of calcite but not the iron minerals. Such postulation, attaching importance only to acidity, creates an erroneous picture. A cave in limestone, for example, could even be formed by neutral solutions, provided that they were not saturated in carbon dioxide at the time of their exit from the ore. Meager data are available on the rates at which solid calcite, siderite, and limonite (amorphous and crystalline) can be taken into solution at different levels of pH and Eh. In the open system of the oxide zone, selective leaching might be more seriously affected by these relative *rates* of solution than by the relative solubilities of these minerals at equilibrium. At present, the writer cannot offer any simple analysis of these leaching effects. They may well represent an interplay of many variables.

Gossan Porosity

GENERAL REMARKS

Where voids are well developed in the leached outcrop of a lead or zinc ore body, their total volume may approximate the volume of sulfides contained in the primary ore prior to leaching. As early as 1926, Augustus Locke noted that there had been no study of the correlation between gossan porosities and primary sulfide contents for the coppez ores:

> Cavities made by the removal of sulfides are mentioned but never with the idea of their systematic variation with the several sulfides from which they come. There are no general data as to whether capping and ore have five or ten per cent of voids, or more, or less.

In the present study, consideration was given to the possible value of gossan porosity as a guide to the grade of hidden ore, with due attention to the many factors other than primary sulfide content which might affect the formation of open voids in a leached outcrop.

At first glance, many gossans are strikingly similar in appearance to the primary ores worked beneath the outcrops, but much of this similarity may be due to the form and distribution of colored iron precipitates rather than to a true cavity reproduction of former sulfides. Only in an unusual case could the total volume of gossan cavities be expected to equal the total volume of leached sulfides. The following are only a few of the many variables which may affect the ultimate porosity developed in a gossan:

1) Filling of voids by limonite. Cavities may be wholly or partially filled by limonite, the actual degree of filling depending on the quantity of iron available in both the gangue and primary sulfide ore minerals, on the acidity developed during oxidation, and on the tendency of gangue and country rock to neutralize this acidity (Nishihara, 1914).

2) Filling of voids by gypsum, silica, and metal oxysalts. The formation of gypsum commonly accompanies the oxidation process, especially if abundant calcium ions are available (as where the gangue is calcite and the bedrock is limestone) for combination with sulfates released on alteration of the sulfides. Such gypsum, if precipitated in the gossan, reduces its porosity. Similarly, supergene silicification of ore outcrops might entirely obliterate void space caused by the leaching of sulfides. Gossan voids may also be occupied by the more insoluble metal oxysalts which tend to accumulate at the surface. Such minerals generally have higher specific volumes than the sulfides from which they are derived, and their filling effects are thus accentuated. With galena, for example, the formation of anglesite involves a 15 to 24 percent increase in specific volume, with cerussite 11 to 17 percent, and wulfenite 6 to 13 percent.

3) Leaching of nonsulfides. Gangue minerals, especially the carbonates, are susceptible to leaching during the oxidation process, and their removal, of course, would tend to increase gossan porosity.

4) Porosity of the primary ore. Primary openings in ore may remain open during oxidation and add to the total porosity in the leached capping. Such "primary porosity" preserved at the surface might introduce a serious error into any estimation of former sulfide volumes by simple gossan porosity determinations. In a prospect area, the porosity of the hidden ore would be an unknown. Ordinary porosity determinations by weighing procedures would merely be a measure of all open and communicated pores, with no distinction as to their mode of origin.

Gossan porosity is, then, a "net effect" of these and other factors, some of which tend to increase, and others to decrease, the formation of open voids in the leached outcrop. Only where the influence of these factors could be judged from the nature of the gossan itself, was there hope of even estimating former sulfide volumes from porosity in the gossan.

A CASE STUDY OF POROSITY AT THE SHINGLE CANYON MINE, NEW MEXICO

To test the possibility that measurements of outcrop porosity may *in some cases* provide a volumetric estimate of the quantity of leached sulfides, an area was sought for study in which: (a) The ore was fairly constant in grade and mineralogy, had low primary porosity, and could be sampled at a shallow depth below the outcrop; (b) the outcrop showed open cavities in place of the leached sulfides, there was little filling of voids by limonite or other materials, and there appeared to be no leaching of gangue.

As expected, these conditions were not found prevailing throughout any single mining district. However, at the Shingle Canyon mine, in New Mexico, some near-surface portions of the ore body fulfilled these requirements. This mine is located 5 miles northeast of Hanover, New Mexico, at the northeastern margin of the zone of mineralization surrounding the Hanover-Fierro quartz monzonite stock. Bedding-plane mineralization just below the contact of the Magdalena limestone (Pennsylvanian) and the overlying Abo shale (Permian) has produced an extensive manto which strikes N. 85° W. and dips 30° N. Ore exposed at the surface terminates down-dip (locally within 80 feet of the surface) against a high-angle fault striking N. 80° E. and dipping about 75° S. Reverse movement on this fault has displaced the manto some 40 feet. The lower, offset part of the deposit has been worked along the lower levels of the mine within the footwall of the fault. The present studies were confined to the shallow workings in the hanging wall, where an almost complete gradation from oxidized to unoxidized ore was accessible. In that part of the ore body selected for the porosity

measurements, fresh sulfides were found at a distance of about 35 feet from the surface down the manto.

The ore body has a fairly constant thickness of from 7 to 8 feet. The ore in the lower 2 to 4 feet occurs as massive layered replacements following bedding in the limestone. Ore in the upper 3 to 6 feet is of lower grade, and the sulfides here occur as selective replacements of fossils within the uppermost part of the Magdalena limestone. The ore in this upper zone is well disseminated and is remarkably uniform in appearance.

An iron-bearing sphalerite (marmatite) was the predominant ore mineral in the deposit. Minor amounts of galena are present, usually as scattered blebs admixed with the zinc sulfide. Varying small quantities of pyrite occur throughout the manto. The gangue consists mainly of unreplaced calcium carbonate and shaly material. Considerable amounts of kaolin were detected by differential thermal analysis of the white gangue. The gangue in that part of the deposit where porosity measurements were made was a hard, dense mixture of silica and kaolin.

The unusually complete selective replacement of fossils by sulfides which characterizes the upper zone of the Shingle Canyon manto can be seen in Plate 6B. In this specimen, marmatite appears as pseudomorphs after fusilinids or as replacements of brachiopod shell fragments. Only the external form of the fossils is preserved. The sulfides also occur as very thin parallel veinlets extending from upper left to lower right across the face of this cut section. An open primary cavity lined with fine quartz crystals occupies the center of this specimen. The white gangue is very hard and consists mainly of silica, with some admixed kaolin and calcium carbonate.

The Shingle Canyon ore body was discovered on the basis of the gossan, which was conspicuous for its red, brown, and black iron and manganese oxide stainings. Furthermore, much of the zinc released on oxidation was retained in the outcrops as zinc carbonate. In the particular area selected for the porosity study, however, only large boulders of the leached, disseminated ore mark the band of outcrop of the ore body at the surface. With oxidation and leaching of the massive sulfides in the lower zone of the ore body, blocks of the upper disseminated ore become unsupported and tend to subside vertically (see fig. 7). Only from the distribution and slumped attitude of these large blocks could one infer the former presence of more massive ore below the gossan that now appears at the surface. Zinc is thoroughly leached from the slumped boulders of disseminated ore. What little lead was present in the original ore has accumulated in the outcrop material and appears as small crystals of cerussite in the gossan voids, or as fine disseminations in the groundmass (presence of the lead-carbonate disseminations was revealed by application of a potassium iodide spray test [Jerome, 1950]). The ground stratigraphically below the leached parts of the

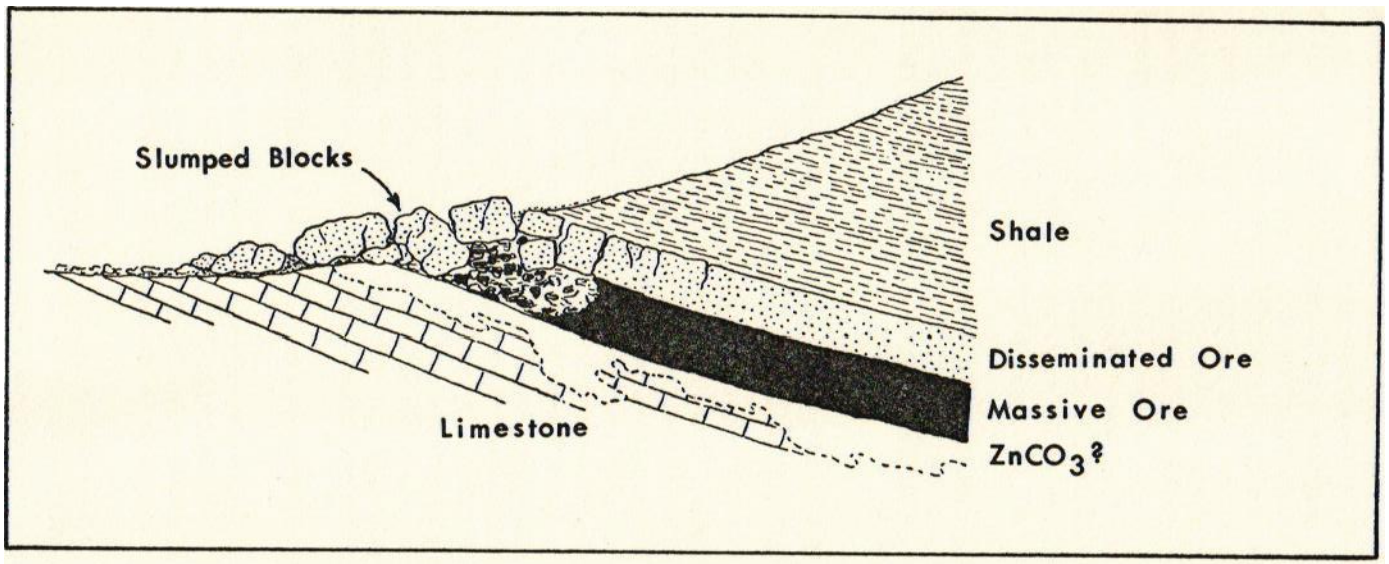

Figure 7

OXIDATION SUBSIDENCE, SHINGLE CANYON, NEW MEXICO

ore body had not been opened; so the quantity of smithsonite "captured" in the underlying limestone is not known.

A cut surface of the gossan material making up the leached boulders of the upper zone is shown in Plate 6A. The cavities are for the most part open, but some are partially filled with cerussite or with goethite, which in places is in the form of poorly developed boxworks after sphalerite. Much of the iron *released* on oxidation of the sulfides has migrated through the neutral siliceous gangue in this area of the gossan and appears as irregular brown stains. The forms of the replaced fossils are still preserved in the shapes of the gossan cavities.

Samples were taken from the leached boulders within a 15-foot interval along the strike of the outcrop, and the corresponding upper zone of the primary ore was sampled over a 15-foot interval along the strike of the ore body directly down-dip from the sample line at the surface. The underground samples were as regularly spaced as the mine workings would allow. The gossan samples were taken from numerous and different spots on the leached ore boulders within the 15-foot strike interval at the surface.

SULFIDE ESTIMATES BY ORDINARY POROSITY DETERMINATIONS

As a first step in the comparison of gossan porosity and leached sulfide volumes at Shingle Canyon, it was assumed that porosity in the capping represents the original porosity of the ore ("primary porosity"), plus the total void space developed by the leaching of sulfides. This assumption therefore attributes the difference in porosity between the original ore and the present gossan wholly to the removal of sulfides and does not take into account the other variables affecting void development and void filling. At first, this assumption *seemed* justified, since at Shingle Canyon the voids appeared to be better replicas of sulfides than in any other area visited and there seemed to be a minimum of void filling by limonite and other oxidation products. To test this assumption, the "leach porosity" of the gossan (total gossan porosity less primary ore porosity) was compared with average figures for the volumetric percentages of sulfides in the primary ore, as they could best be determined.

Primary ore porosities were determined by a method described in Appendix C.

The porosities of gossan samples were obtained by a series of simple weighings: The sample dry in air (W_1), the sample saturated in water (W_2), and the sample water-saturated in air (W_3). The percent porosity (if measurements are made in metric units) is then given by the formula:

$$\frac{W_3 - W_1}{W_3 - W_2} \times 100 = \% \text{ porosity.}$$

Saturation of samples was accomplished by gentle boiling for 10 minutes and was tested by splitting the sample after the determination to confirm interior wetting. The samples were dried and reweighed to determine the amount of material lost in boiling. Although the latter proved negligible in the case of the siliceous gossan samples from Shingle Canyon, it might lead to considerable error if more friable or soluble materials were tested by this procedure. Repeated tests on the same samples checked to within 2 percent porosity.

Volumetric percentages of sulfides in the primary ore samples were measured by microscopic counts (discussed below) and checked by calculation of sulfide volumes from assay returns (as outlined in appendix D). The figures obtained for total gossan porosities, primary-ore porosities, and volumetric percentages of primary sulfides are listed in Table 3.

A comparison of the values in columns A and C of Table 3 will show that figures for total gossan porosity (mean 26.4) are considerably lower than the volumetric percentages of sulfides in the primary-ore samples (mean 32.2). Since primary-ore porosity (as high as 15 percent) must be

TABLE 3. SULFIDE ESTIMATES BY GOSSAN POROSITY DETERMINATIONS

ESTIMATES BY ORDINARY METHODS OF POROSITY DETERMINATION			ESTIMATES BY APPLICATION OF MICROSCOPIC COUNTS TO GOSSAN VOIDS	
(A)	(B)	(C)	(D)	(E)
% gossan porosity	% primary ore porosity	Vol. % primary sulfides	Vol. % sulfide cavities	Vol. % primary sulfides
(1) 30.6	(1) 3.3	(1) a– 31.0	(1) a– 34.0	(1) a– 31.0
(2) 24.3	(2) 6.7	b– 34.2	b– 36.3	b– 34.2
(3) 27.6	(3) 8.1	(2) a– 29.9	(2) a– 37.9	(2) a– 29.9
(4) 25.7	(4) 10.5	b– 35.6	b– 39.4	b– 35.6
(5) 27.9	(5) 3.9	(3) a– 27.1	(3) a– 32.6	(3) a– 27.1
(6) 26.2	(6) 10.9	b– 30.1	b– 31.1	b– 30.1
(7) 27.2	(7) 2.3	(4) a– 37.3	(4) a– 32.8	(4) a– 37.3
(8) 21.3	(8) 8.2	b– 36.0	b– 38.2	b– 36.0
	(9) 15.1	(5) a– 28.7	(5) a– 33.8	(5) a– 28.7
	(10) 8.3	b– 32.6	b– 30.8	b– 32.6
	(11) 12.5	(6) 32.3	(6) a– 31.1	(6) 32.3
	(12) 10.0	(7) 32.4	b– 29.0	(7) 32.4
			(7) 34.0	
			(8) 31.0	
			(9) 30.0	
			(10) 28.0	
			(11) 20.1	
$n = 8$	$n = 12$	$n = 12$	$n = 17$	$n = 12$
$\bar{x} = 26.4$	$\bar{x} = 8.3$	$\bar{x} = 32.2$	$\bar{x} = 32.4$	$\bar{x} = 32.2$
$s = 2.57$	$s = 3.66$	$s = 3.10$	$s = 4.55$	$s = 3.10$

n = number of samples.
$\bar{x}$ = arithmetic mean.
s = standard deviation.

subtracted from total gossan porosity for the estimation of cavities due to the leaching of sulfides, it is apparent that predictions of sulfide volumes from measured leach porosities would be inaccurate. The fact that the leach porosities are consistently lower than the original sulfide volumes merely reflects the fact that voids resulting from sulfide leaching do not remain completely empty during oxidation. The appearance of the Shingle Canyon gossan was deceptive in that cavity filling seemed to be negligible. Actually, the degree of filling introduced a serious discrepancy between sulfide volumes and total voids after sulfides.

The writer is convinced that ordinary gossan porosity determinations cannot be used to predict original sulfide volumes. Use of the method outlined above shows that there is no correlation in the case of the Shingle Canyon gossan, even though this was purposely selected for analysis because of its unusual selective leaching of sulfides and the open appearance of its voids. A correlation would be even less probable in deposits where void filling is apparent and gangue minerals as well as sulfide minerals are subject to leaching. From the practical standpoint, such determinations can be rejected at the start because they presuppose a knowledge of primary-ore porosity. As pointed out in the preceding section on factors affecting void development, primary-ore porosity would be as much of an unknown as primary-sulfide volumes when dealing with an unexploited outcrop for which there were no subsurface data.

APPLICATION OF MICROSCOPIC COUNTS TO THE MEASUREMENT OF GOSSAN VOIDS

In view of the difficulties encountered in attempting to correlate measured leach porosities with sulfide volumes, a new method of porosity determination was developed. This technique permits direct measurement of the total volume of gossan cavities formerly occupied by sulfides whether at present open or filled. Where gossan voids due to sulfide leaching can be distinguished under the microscope from original primary pores, sulfide estimates can be made "from the surface" without previous knowledge of primary-ore porosity.

The method of making such a quantitative estimate is a modification of the standard Rosiwal count used in the determination of mineral volumes in rocks by means of linear microscopic traverses over thinsections. The Rosiwal method is based on the principle that the linear percentage of any rock component is equal to its three-dimensional percentage in the rock.

The first step in the procedure is the selection in the field of representative samples of gossan from the ore outcrop. Several thick (3- to 5-mm) sections are then cut at random from each sample with a diamond saw. The thickness of the sections will depend on the friability

of the gossan material under study. Impregnations of the specimen with Canada balsam or Lakeside cement may be necessary if the material is especially fragile.

Each cut surface is mounted on a mechanical stages and viewed through the microscope in reflected light. The procedure is similar to that for a standard Rosiwal count of a petrographic section (Holmes, 1930; Larsen and Miller, 1935). With the help of the stage, a traverse is run across the cut surface, and simultaneously a count is made of the number of points at which the cross hairs fall on sulfide cavities and the total number of points in the traverse. At the end of each traverse, the section is mechanically moved to the next adjacent traverse, and another count is made. According to Holmes, for a statistically valid analysis, the total length of traverse must equal at least 100 times the average diameter of the apertures measured. In the present study, this was checked by plotting cumulative volumetric sulfide percentages against the cumulative length of traverse at each shift to a new line of traverse (fig. 8). The counts were continued until the cumulative average of sulfide cavities in each section became constant. The number of points counted for each section of the Shingle Canyon gossan varied from 1,300 to 3,000.

This method offers a reliable means of estimating the volumetric percentages of sulfides formerly present within a given gossan specimen taken at the surface. Whether or not it can be used successfully to obtain an approximate estimate of the original sulfide content in a gossan as a whole depends on the homogeneity of the original ore and the sampling technique applied.

Microscopic counts were applied to the Shingle Canyon gossan. Eleven samples taken within the 15-foot interval at the surface were analyzed. Two sections from each of 6 of these samples were counted, and 1 from each of the remaining 5 (table 3, column D). In these traverses, primary openings were excluded from the sulfide-cavity count. They were recognized as lacking the iron staining and poorly developed boxworks present in voids after sulfides. Some of the primary voids were lined with fine growths of drusy quartz.

The volumetric sulfide percentages listed in columns C and E of Table 3 were also determined by microscopic point counts. Two sections from each of 5 samples were counted, and **1** from a fifth. Entry 7 in column E represents a volumetric percentage of sulfides calculated from assay returns and density measurements on three samples that were pulverized, quartered, and subjected to wet analysis on iron and zinc. This calculation is shown in Appendix D.

The volumetric percentage of sulfides **in** the shallowest unoxidized ore at Shingle Canyon was taken as the standard for comparison with the sulfide-cavity estimates made at the surface. The uniformity of the ore

3. A Chayes point counter was used in the present work. The operation and accuracy of this stage is discussed by Chayes (1949).

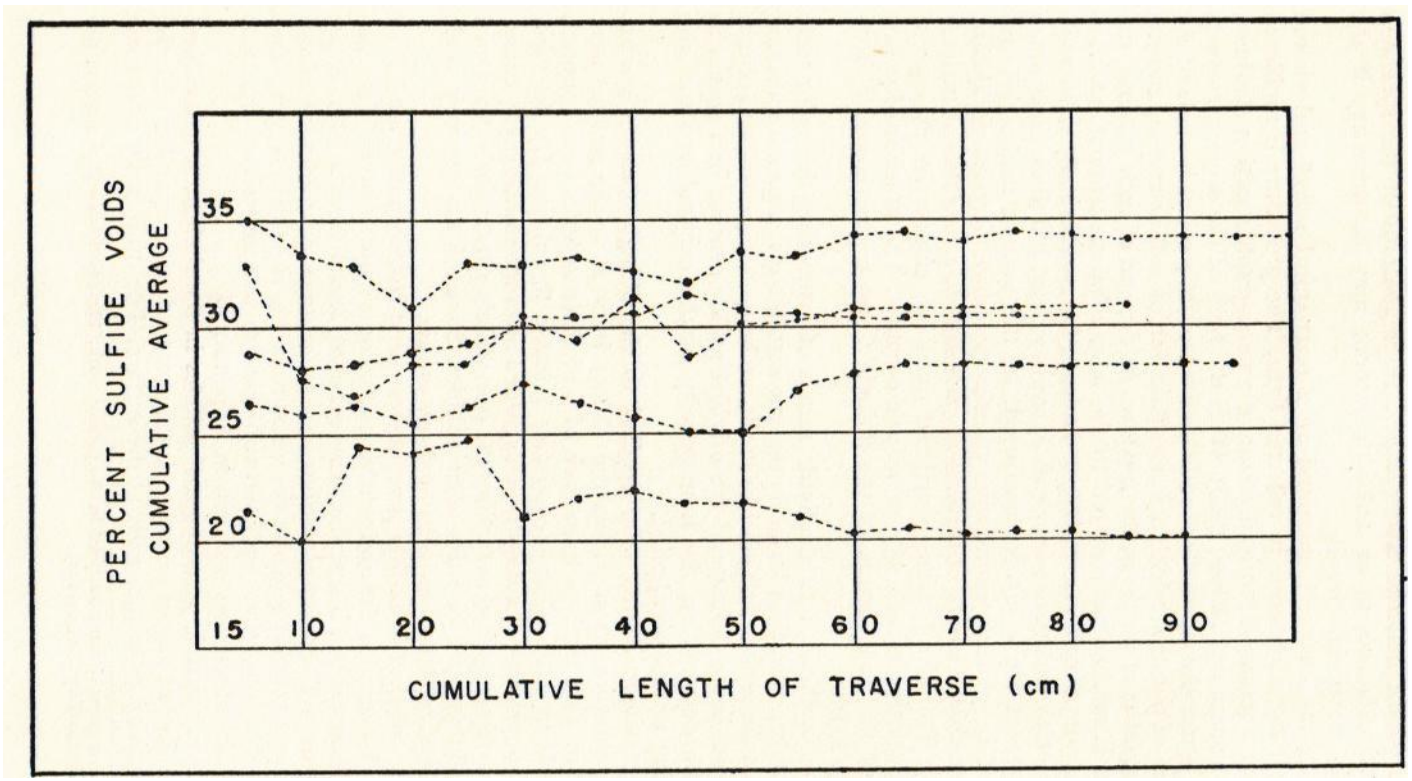

Figure 8

MICROSCOPIC ESTIMATES OF SULFIDE VOLUMES, SHINGLE CANYON, NEW MEXICO

in the manto led to the belief that the ore once present in outcrop was not significantly different from the ore now found in the shallowest underground workings. There is no way to prove this conclusively.

The mean for sulfide-cavity estimates (32.4%) fell very close to the mean for sulfide volumes in the ore samples analyzed (32.2%), suggesting the value of the microscopic technique from a prospecting standpoint. The difference in these means should be considered more critically. The fact that the difference is so small is coincidental, but the true difference can be said to lie within 3 percent with 95 percent accuracy.[4]

LIMITATIONS OF THE MICROSCOPIC METHOD

The microscopic method is applicable only to leached outcrops with small, discrete sulfide cavities. Since the traverse necessary to obtain reliable estimates is at least 100 times the diameter (mean) of the sulfide cavities, the dimensions of the mechanical stage place a limitation on the size of the sulfide cavities which may be considered, to say nothing of the time involved in excessively long microscopic counts. Fortunately, however, the problem of accurate sulfide estimates is acute only in the case of the lower grade ore outcrops, and in these the sulfide cavities are generally small.

The microscopic technique might be profitably applied to leached outcrops over the disseminated porphyry-type copper ores. In these, voids after sulfides are generally small and discrete and could be readily distinguished from the "porphyry" groundmass. Primary pores should be readily recognizable as minute cracks and microvugs. In addition to providing a direct measure of protore sulfide content where applied to such ores, this technique might have the added value of suggesting especially favorable ground for supergene enrichment. For example, the greatest abundance of secondary sulfides might be expected in drainage areas under those portions of a capping having the greatest measured abundance of sulfide cavities.

4. A variance-ratio test, assuming normality, gave an F-value of 2.16, which, for the degrees of freedom involved, established no significant difference in the variances on a .01-probability level. The standard error of the mean of the two samples, based on a pooled estimate of the variance, was found to ***be*** 1.56.

Outcrop Colors as Guides to Lead and Zinc Ore

PREVIOUS STUDIES

Past studies by other investigators, especially of the porphyry-copper ores of the Southwestern United States, have shown that the colors of iron precipitates in a leached outcrop are in some cases moderately reliable indicators of the types and quantities of sulfides originally present.

Blanchard (1939a) and Tunell (1930) agree in assigning "a deep maroon to seal-brown color" to cappings over chalcocite ore. Blanchard reported that "limonites derived from chalcopyrite frequently show a deeply ochreous color, and at other times an Indian red." An example of the practical application of color criteria is provided by the Bagdad porphyry-copper deposit, where the boundary at the surface between leached ore and leached protore was recognized on the basis of color differences alone (Anderson, 1950).

Blanchard and Tunnell realized that the factors affecting outcrop colors are manifold and may limit the reliability of color as a guide to ore. Grain sizes of the limonite, degree of packing, orientation of crystallites, presence of impurities, and surface coatings are only a few of the variables other than primary mineralogy which may affect the colors seen in a gossan. It is known, however, that the colors of synthetic hydrous ferric oxides reflect the various chemical conditions under which the colloidal iron particles are initially precipitated (Weiser, 1926). This fact lends credence to the idea that differences in limonite colors might be traced back, in some cases, to differences in the original ores from which the ferric oxides are derived.

The occurrence of color guides was realized by Locke (1926), who stated that:

> From the beginning of the study of outcrops, there was noticed a variation of color with the sulfides from which the iron precipitate was derived. In extreme cases, this was so marked as to serve for the selection of good ground. In view of the complicated factors which in general contribute to the production of a given color, such a result is contrary to expectation.

The colors in iron cappings over lead and zinc ore deposits have received little attention compared to the work done with the copper-iron bodies. Notable exceptions are the studies of Blanchard and Boswell (1927) and Harrison Schmitt (1939). Blanchard and Boswell found that the rectangular cleavage boxworks after galena were commonly

composed of an "ochreous-orange" limonite (visible on fresh surfaces) and offered this as a possible criterion for lead. On weathered surfaces, this color is purported to change to a "seal-brown" or "dark chocolate." The color on freshly broken surfaces can be distinguished from the fine cellular limonite of chalcopyrite origin by "its deeper orange tint, and a certain velvety, rather than pulverulent, slightly coalesced appearance."

From a careful examination of gossan tappings over the zinc ore bodies at the Hanover mine, New Mexico, Schmitt observed that the iron precipitates after gangue (salite) are a "kaiser brown" and commonly preserve the mineral's radiating crystal structure, whereas limonite after sphalerite is "ochreous-orange" (see description of this property). Schmitt mentioned that gangue and sulfide areas could be distinguished on this basis, and that a close estimate (±S%) of former sulfide content could be made visually by an experienced observer. A significant innovation by Schmitt was the use of color charts for the standardization of his descriptions. Where subtle color differences are involved, it is most difficult to convey an accurate picture of a given color without some such control.

PRESENT STUDIES

PROCEDURE

The significance of the outcrop colors over lead and zinc ore bodies examined in the course of the present study was tested by describing the characteristic limonite colors for each area and by comparing their variation with changes in primary ores from district to district.

All descriptions were standardized by use of the Goddard Rock-Color Chart.[5] Other color charts might have been selected for this work, but the Goddard chart was chosen because it permits simple, rapid, and fairly accurate field determinations of the hue, value, and chroma of any given color.

The colors of indigenous iron oxides most commonly found in the voids after a particular sulfide were considered as representative of that sulfide. The sulfide cavities themselves were identified by void shapes, by boxwork structures, or by the presence of indicative minerals such as cerussite, wulfenite, and hemimorphite when localized to certain cavities or associated only with iron precipitates of a certain color. In each area, the mineralogy of the primary ore was known.

All observed colors are listed by district in Table 4. These are descriptions of the iron precipitates only. The meaning of colors characteristic of certain nonferric minerals such as pyromorphite, aurichalcite, and wulfenite is self-evident in any outcrop.

5. A rock-color chart prepared in 1948 by a committee (E. N. Goddard, chairman) of the National Research Council. This chart can be purchased from the Superintendent of Documents, Washington 25, D. C.

TABLE 4. OUTCROP COLORS

LOCALITY	PRIMARY ORE	OUTCROP COLOR	COLOR KEY
New Mayberry mine, Bingham, Utah	Pyrite	Grayish red to moderate brown	10R 4/2 to 5YR 3/4
	(Gangue)*	Dark yellowish orange	10YR 6/6
	Galena	Moderate reddish brown	10R 7/6
Capote mine, Sonora, Mexico	Pyrite	Dark reddish brown	10R 3/4
	(Gangue)	Dark yellowish orange	10YR 6/6
Grant County mine, New Mexico	Pyrite	Dusky red to very dusky red	5R 3/4 to 10R 2/2
	Sphalerite	Moderate brown	5YR 11/12
	(Gangue)	Dark yellowish orange	10YR 6/6
Shingle Canyon mine, New Mexico	Sphalerite	Light to moderate brown	5YR 5/6 to 5YR 4/4
Grasselli mine, Tennessee	Sphalerite	Light brown	5YR 6/4
	(Gangue)	Very pale yellowish orange	10YR 3/2
Davis mine, Tennessee	Sphalerite	Light brown	5YR 6/4
	(Gangue)	Very pale yellowish orange	10YR 3/2
Pewabic mine, Hanover, New Mexico	Pyrite	Moderate brown	5YR 3/4 to 5YR 4/4
	(Gangue)	Dark yellowish orange	10YR 6/6
	Sphalerite	Light brown	5YR 5/6
	(Gangue)	Grayish brown	5YR 3/2
Anita mine, Lordsburg, New Mexico	Sphalerite	Dark yellowish orange	10YR 6/6
	Galena	Moderate reddish brown	10R 4/6
Atwood mine, Lordsburg, New Mexico	Sphalerite	Dark yellowish orange	10YR 6/6
	Galena	Moderate reddish brown	10R 4/6
Providencia mine, Zacatecas, Mexico	Sphalerite	Dark to moderate yellowish orange	10YR 6/6 to 10YR 7/6
	Galena	Very dusky red to dusky reddish brown	10R 2/2 to 10R 3.5/4
Lark vein, Bingham, Utah	Sphalerite	Dark yellowish orange to light moderate brown	10YR 6/6 to 5YR 11/12
	Galena	Same as ZnS color	

TABLE 4. OUTCROP COLORS (continued)

LOCALITY	PRIMARY ORE	OUTCROP COLOR	COLOR KEY
Hidden Treasure mine, Ophir, Utah	Sphalerite	Light yellowish brown	7YR 6/6
	Galena	Same as ZnS color	
Luna mine, Apache Hills, New Mexico	Sphalerite	Light brown	6YR 5/6
Ford prospect, Apache Hills, New Mexico	Galena	Blackish red	5R 2/2
Last Chance mine, Apache Hills, New Mexico	Galena	Very dusky red	10R 2/2

* If gangue is limonitized to a characteristic color, it is also listed (e.g., gangue limonitized by iron from pyrite).

COLORS ASSOCIATED WITH SPHALERITE

The presence of sphalerite in a primary ore leads most commonly to the formation of light to moderate browns (5YR 6/4 to 5YR 4/4 to 6YR 5/6) or moderate yellowish oranges (10YR 7/6) in the outcrops. Sphalerite derivatives unfortunately show great variety in color and may even vary within a single district. At the Grant County mine, near Hanover, New Mexico, for example, large cavities after sphalerite are found at the surface in limonitized chloritic shale, and these cavities are lined by a fine dusky-red coating of iron oxides. Elsewhere in the same area, the more common light moderate brown after sphalerite appears. The application by Schmitt of a sphalerite color criterion at the Hanover mine has already been discussed. The writer assumes that he has observed the same colors for sphalerite as those recorded by Blanchard and Boswell, which they are said to have described as "light brown and brownish" (Bateman, 1950, p. 258-259), though such wording could not be found in the original publications on zinc derivatives by Blanchard and Boswell.

COLORS ASSOCIATED WITH GALENA

From the present studies, it appears that a dusky red (10R 2/2) to dusky reddish brown (10R 3.5/4) is characteristically associated with outcrops formerly containing lead. The "ochreous-orange" lead color described by Blanchard and Boswell was seen in two districts: over the Lark Vein at Bingham, Utah, and in the gossan of the Hidden Treasure mine, Ophir Hill area, Utah. In those localities, however, the same color was seen in sphalerite boxworks, and there, at least, it appears to lack diagnostic value. Blanchard and Boswell have noticed "dull reddish browns" after galena where there is a pronounced predominance of pyrite. In the present study, this color was found in association with lead outcrops, but apparently independent of large amounts of pyrite.

COLORS ASSOCIATED WITH PYRITE

The widespread recurrence of similar color patterns in the gossans of different districts was most frequent in the case of pyritic outcrops. Such outcrops are generally a very dusky red (10R 2/2) to dark reddish brown (10R 3/4) to moderate brown (5YR 4/4) in sulfide void areas, and dark yellowish orange (10YR 6/6) in limonitized gangue areas. This description applies to sulfides in fairly active gangue capable of precipitating the yellowish-orange precipitates in the immediate area of the pyrite source. Where pyrite is oxidized in more inert gangues, the yellowish-orange precipitates are absent or less abundant.

In shales (as at the Grant County mine, New Mexico) or in limestones (New Mayberry mine, Utah), the gangue is limonitized and stands out in marked contrast to the reddish-brown void areas. The outcrops over the pyritic Grecian Bend ore body of the New Mayberry mine (Bingham district, Utah) may be cited as an example of color variations due to gangue. Pyrite in this area occurs in both limestone and quartzite. At the surface, the pyrite-carbonate ore has the distinctive pattern described above: reddish brown at former sulfide sites and dark yellowish orange in limonitized gangue areas. The removal of iron from the inert siliceous ore, however, is almost complete, and the porous sponge of residual silica is merely stained grayish red (10R 4/2) throughout. Locally, minor amounts of the dark yellowish-orange limonite are precipitated where reaction has presumably taken place between the iron-bearing solutions and waters introduced from the nearby limestones. A considerable amount of iron removed from the oxidized siliceous ore is trapped as limonite of the "fluffy type" (Blanchard, 1939) in the limestone. The colors of these latter precipitates vary with the purity of the limonite, but are in general a moderate yellowish orange (10YR 7/6).

At the Pewabic mine (Hanover, New Mexico), pyrite occurs disseminated through altered granodiorite dikes, which, when oxidized at the surface, present the same color pattern produced in other areas by pyrite in carbonates. Here, much of the dark yellowish-orange limonite in the gangue areas was produced by the gangue itself (mainly an iron-rich chlorite, thuringite).

Table 4 lists only those areas where there seemed to be a correlation between outcrop colors and former sulfides. In some of the mining districts visited, no such relationship could be worked out. At the Bullfrog mine (Vanadium, New Mexico), for example, the inert quartz gangue and igneous wall rocks of the zinc veins have promoted the migration of iron and manganese oxides to such an extent that the distribution of colors in the outcrops reflects more the course and degree of transportation of these oxides than it does the original distribution of sulfides. Only the characteristic pyrite color pattern was found in this

area, whereas no colors could be established for the lead or zinc ore known to occur in the veins.

COLORS OF TRANSPORTED OXIDES

The distinction of transported from indigenous iron oxides is more readily made by studying the form, rather than the color, of the iron precipitates. In this study, as in others, transported oxides were found to vary greatly in color, and occurrences of reddish, yellow, brown, and even irridescent limonites side by side in a single hand specimen were not uncommon. The best present criteria for transportation are the limonitic textures and structures described by Blanchard and Boswell in several of their papers on the limonite derivatives. Although attention was given to transported limonite colors in the present study, no significant variations with differing sulfide sources were observed in any area.

CONCLUDING STATEMENT

In some of the areas visited, the colors of indigenous iron precipitates in the outcrops bore a definite relation to original lead, zinc, and iron sulfides. 'Where this was the case, the colors associated with each sulfide were recorded by use of a standard color chart. These colors are, in general, dusky reds for galena, light browns to yellowish oranges for sphalerite, and dusky browns to reddish browns for pyrite. Where pyrite has oxidized in a reactive gangue, the dusky brown to dark reddish brown of the indigenous oxides may be accompanied by yellowish-orange limonite in the stained or replaced gangue areas adjacent to the voids.

From Table 4, it is apparent that no one gossan color or color pattern was found in the areas studied which can be regarded as universally diagnostic of the former presence of lead or zinc in the outcrops. A color indicative of ore in one area may be insignificant or entirely absent in another. In view of the many complicating factors which may affect the colors seen in a leached outcrop, this lack of general criteria is understandable. Color may be *locally* significant because these complicating factors, such as the composition of gangue and country rock, climate, rainfall, and drainage, are *locally* constant. The discovery of useful color criteria is therefore a task for the geologist acquainted with the local mining area. General observations such as those recorded in the present study and in the valuable papers of Blanchard and Boswell may be of assistance in this task, but should not be applied indiscriminately without allowance for local variations.

Appendix A

FEATURES OF OXIDATION IN AREAS VISITED FOR SAMPLING

PEWABIC MINE, HANOVER, NEW MEXICO

Location: One-half mile east of the town of Hanover, southeastern New Mexico.

For a detailed description of the Pewabic mine, the reader is referred to an excellent paper by Harrison Schmitt (1939). Surface and underground workings of this mine are in the southeastern part of the zone of pyrometasomatism surrounding the intrusive Hanover-Fierro (quartz-monzonite) stock.

The ores are worked exclusively for their zinc; they contain little copper and practically no lead. Oxidized outcrops of the ore exposed in an open pit (Pewabic quarry) at the southern end of the property were considered for the gossan study. Here, thoroughly oxidized ore could be traced into fresh sulfides within a foot or two, and there was no difficulty in correlating gossan and primary ore.

The Pewabic quarry lies within a skarn zone close to the quartz monzonite stock, and sphalerite, the ore mineral, is most commonly associated with ilvaite, salite, and pyrrhotite. The ore is localized by vertical preore northeast fractures and occurs as irregular sphalerite replacements of preexisting silicates.

Three distinct types of gossan are found in this area:

(I) Gossan associated with the zinc ore. A thin (0- to 10-ft) iron capping is developed over the lead-free zinc ores of the Pewabic mine. The oxidation is shallow, because of the dense, impermeable nature of the ore (porosity 0.7 to 1.5 percent), and abundant relict sulfides may be found at, or close to, the surface throughout the area.

Most commonly, the sphalerite is found as scattered veinlets and blebs cutting across and replacing radial aggregates of salite. Schmitt (1939) has described the preservation of these structures in the gossan limonites at the nearby Hanover mine, on the western side of the intrusive. There, the iron oxides derived from the gangue and those from the sulfides differ in color and structure (fig. 9) and permit a visual grading of the original ore. Limonite after salite is dark brown and preserves the mineral's radiate acicular form, whereas the sphalerite produces limonite of a lighter brown color and lacking pronounced structure. At the Pewabic mine, this distinction of limonite types may be made locally with a hand lens, but is not characteristic. The silicates are finer grained, and it is difficult to distinguish former sulfide areas

in the oxidized ore. Relict marmatite is exposed at the surface in the area just to the north of the Pewabic mine offices, but in the Pewabic quarry, to the south, fresh sulfides are concealed below the leached capping. As a whole, the Pewabic zinc gossan is indigenous and has proven a reliable guide to the area of ore formerly existing in the plane of the present surface.

(2) Gossan associated with magnetite bodies. Irregular deposits of magnetite also occur within the contact zone of the Hanover-Fierro stock (Paige, 1909). They vary greatly in size and are composed of fairly pure, massive Fe_3O_4. One such body cropped out in the Pewabic quarry.

Where exposed, this deposit has altered to goethite (FeO • OH) and

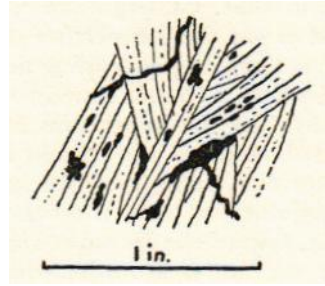

Figure 9

ZINC GOSSAN OF THE HANOVER MINE, NEW MEXICO (FROM SCHMITT, 1939)

Sketch showing radial structure in limonite after saute gangue, and irregular patches and veinlets of limonite after sphalerite (in black).

shows delicate boxworks of the limonite formed in partially decomposed magnetite (pl. 7A). Fine limonite fillings along fracture and parting planes emerge as a subrectangular system of ridges on removal of the Fe_3O_4 matrix. This boxwork lacks the intricate structure developed along the pronounced and detailed cleavage planes in galena. Furthermore, it is extremely fragile, by reason of the thinness and poor connection of the goethite ridges, and is destroyed by continued weathering.

The iron capping over the magnetite consists of laminated (shelly) limonite, suggesting transportation of the iron before its precipitation in the gossan. Fragments of this limonite contain very small amounts of unaltered magnetite and, unlike the zinc derivatives, are attracted to an ordinary alnico magnet.

(3) Gossan associated with pyrite deposits. Exposure of a pyrite gossan (pl. 7B) was seen just south of the Pewabic quarry where a pyritized and chloritized dike transects upper Magdalena limestone. Fresh, cubic pyrite embedded in a groundmass of fine-grained thuringite within the dike was intersected in diamond-drill holes at depths of from 60 to 80 feet.

On weathering, the iron-rich chlorite is completely limonitized, and no relicts of the original mineral are preserved at the surface. The pyrite is leached, forming open cavities with almost perfect cubic shapes. These voids are lined with fine coatings of irridescent or dusky-brown limonite.

GRANT COUNTY MINE, NEW MEXICO

Location: Three-fourths of a mile east of the Pewabic mine, east of Hanover and north of Santa Rita, in southwestern New Mexico.

The Grant County mine was in its preliminary stages of development when examined in 1951. Underground workings at a depth of about 150 feet exposed ore at the intersection of a preore porphyritic granodiorite dike with major, steeply dipping northeast fractures. Vertically, the ore is confined to a 15-foot zone in the favorable Hanover limestone and is "roofed" by the impervious Mountain Home shale. Surface drilling 100 yards south of the present mine workings proved that mineralization continues along the dike in that direction but is mainly pyritic. Throughout the area, the ore is found only on the western side of the dike, toward the Hanover-Fierro intrusive stock.

Underground, the ore varies from massive iron-rich sphalerite (marmatite), along the preore northeast fractures, to a typical "kidney ore" away from the fractures, where the marmatite appears as rounded isolated masses in epidotized and chloritized limestone. The groundmass of the ore is light to dark green, owing to the abundance of chlorite, the chief gangue constituent and principal alteration mineral. Minor amounts of pyrite are associated with the zinc ore, but, as previously mentioned, pyritization is much more prominent in the unopened ground south of the present working.

Among the more interesting features of the Grant County mine is the phenomenon of ore "leakage," as discussed by Harrison Schmitt in 1939. Although the underground ore shoots generally terminate upward against an impervious, or at least inert, flat-lying shale, some ore has found its way up into the overlying formations along the preore dike. As a result, weak, "spotty" shows of gossan are found within 50 feet of the dike along the present surface. The presence of this "spotty gossan" in the unfavorable horizon exposed at the surface is a guide to more intense mineralization concealed in more favorable sediments along the dike at depth. Schmitt has shown that with an awareness of this structural habit of the ore and a knowledge of the regional stratigraphy, the location of workable sulfides below weak surface "leakages" can be predicted with accuracy.

Naturally, the "leakage" gossan is not representative of massive sulfides but occurs as scattered patches of porous red to brown iron oxides in a groundmass of dark yellowish-orange limonite. Actually, the surface is covered by 2 to 3 feet of fragmental rock float, but the

gossan was exposed in a roadcut, in a prospect pit, and in a 100-foot sample trench dug in a direction normal to the northward trending dike contact.

The porous limonites of the zinc gossan lack any definite characteristics of a sphalerite derivative. The cellular structure is irregular, but in places large open cavities, 1 to 3 cm in diameter, are lined with reddish iron oxides; their general appearance is similar to the "kidney ore" found underground, and these cavities are therefore presumed to have originally contained sphalerite.

Additional pyritic gossan found over the drilled but unopened ground south of the present workings had many definite cubic voids which aided in the identification of the original sulfides. The chloritic groundmass in the pyritic gossan is thoroughly altered to a dark yellowish-orange limonite.

BULLFROG MINE, VANADIUM, NEW MEXICO

Location: At Vanadium, in the Bayard district, Central mining area, New Mexico; southwest of Santa Rita, northeast of Silver City.

Outcrops of the lead-zinc veins of the Bullfrog mine were inspected in 1952. On this property, steeply dipping siliceous veins bearing variable amounts of sphalerite, galena, chalcopyrite, and pyrite occur in granodiorite and shale, and locally along the margins of granodiorite and quartz monzonite dikes which predate the ore. Sphalerite is the chief ore mineral and is accompanied by lesser amounts of galena and negligible quantities of chalcopyrite. Gangue consists mainly of quartz, chlorite, and rock breccia fragments of different sizes. There is a complete gradation from massive sulfide ore to complete vein filling by gangue matter. The walls of the veins have been pyritized and strongly chloritized. Locally they are bleached. The workable thickness of ore varies from 1 to 5 feet over short distances but averages about 2 to 3 feet. Production has come exclusively from fresh or only partially oxidized ore. For additional data on this mine, the reader is referred to a summary by Lasky and Hoagland (1948).

The transition at depth from oxidized to unoxidized ore in the Bullfrog mine is generally well within 100 feet of the surface—shallow enough to have been affected by surface irregularities. The maximum topographic relief over the veins is only 130 feet but is more than sufficient to expose unoxidized ores in the valleys. From 60 to 90 feet of oxides is preserved over the veins in higher ground, but erosion has kept ahead of oxidation in the intermittent stream valleys. Quartz-sulfide stringers containing sphalerite, and subordinate pyrite and galena, were found in the outcrops along Gold Gulch, the main valley in the area, during the early mining days (Lasky, 1936).

Where quartz-sulfide ore was once exposed in higher ground, leached masses of bold white quartz can be followed along the vein outcrops.

Cavities and fractures within this quartz are coated with black to brown to reddish iron oxides, and tabular crystals of wulfenite are abundant within the voids. The lead molybdates are a surface accumulation and die out about 10 feet below the surface. The primary ore contains only about 0.5 to 1.0 percent Pb, but because of the residual concentrations of wulfenite, the siliceous outcrops assay up to 3 percent Pb. No cerussite or anglesite was found in the gossan, which was thoroughly leached of zinc. Very little limonite of the cellular variety is found within the inert quartz gangue left at the surface.

The outcrops are not particularly prominent over the more productive parts of the veins, but to the west (as along the barren parts of the Old Slate vein), where the quartz gangue is dominant and the sulfides diminish, vertical bold quartz ridges stand as high as 12 feet over the veins.

Ore of the breccia type, in which angular fragments of country rock are cemented by sulfides, can be readily reconstructed from their oxidized and leached equivalents at the surface. The breccia structure is preserved; the irregular rock fragments, stained and marginally replaced by iron oxides, appear embedded in a matrix of porous boxwork structures.

ANITA MINE, NEW MEXICO

Location: One mile west of Shakespeare and Veladon, in the Lordsburg mining district, New Mexico.

The outcrops of the Anita mine (Lasky, 1938) were briefly examined in the summer of 1952. At the time of the writer's visit, the mine was not in operation, and its workings were inaccessible, but samples were taken from the old dumps and from the leached ore outcrops.

This mine exploited a steeply dipping silver-lead-zinc vein in granodiorite and basalt. The ore contained various quantities of galena, sphalerite, chalcopyrite, and pyrite in a gangue that was chiefly quartz, with small amounts of barite, fluorite, and calcite. The precious-metal content averaged .07 to .09 oz Au and 9.7 to 11.1 oz Ag per ton. The vein, which has a mean width of 5 feet, was oxidized to a depth of 800 feet, and much lead carbonate was mined in place.

The outcrop of the vein is composed mainly of preserved hypogene quartz and is slightly more prominent (topographically) than the basalt and granodiorite wall rocks. Leached cavities in the preserved vein matter are lined with red and yellowish iron oxides; cellular limonite is not well developed. The reddish oxides appeared to be associated with wulfenite, whereas the yellow coatings occur in cavities free of wulfenite. A great variety of minerals were found in dump specimens. These include cerussite, anglesite, wulfenite, malachite, azurite, aurichalcite, chalcocite, covellite, and hemimorphite. Only wulfenite,

however, was found in place at the outcrop. The writer can say nothing from firsthand experience of the distribution of oxides underground.

PROVIDENCIA MINE, MEXICO

Location: Near the town of Avalos, Zacatecas, Mexico, about 106 miles southwest of Monterrey, Nuevo Leon.

The Providencia mine of the Peñoles Mining Company has long been a productive source of high-grade lead-zinc ore. The ore occurs in almost vertical chimneys in steeply dipping Jurassic limestones very near, and locally in contact with, a quartz monzonite intrusive. In the upper levels of the mine, the mineralization has been controlled chiefly by bedding (which strikes N. 55° W. and dips 70° SW.), and the ore is confined to single strata. In the lower levels (below level 10, depth ca. 3,300 feet), the ore chimneys are elongated in the direction of pronounced fractures striking N. 30° E. and dipping 70°-80° E. (Triplett, 1952).

The principal sulfides are pyrite, galena, and sphalerite. Rhodocrosite, calcite, and quartz make up the gangue matter. In places, the chimneys are solid sulfide masses which contain unusually large amounts of pyrite.

The oxidation of these ores has extended to a depth of over 1,200 feet. The level of transition from oxidized to unoxidized ore was controlled by a high Tertiary or post-Tertiary stand of the water table, whose natural level is now 1,300 feet below the transition and 2,500 feet below the present surface. Evidence of this earlier high stand of the water table was cited by W. H. Triplett, who showed that there is a slight enrichment of silver and gold in the primary sulfide zone directly beneath the transition zone.

Although this ancient stand of the water table controlled the general level of transition from oxide to sulfide ore, the undulations in that transition have been determined by the degree of fracturing of the country rocks and ore. The ore chimneys in more highly fractured zones of greater recharge have been more deeply oxidized than ore bodies in more impervious ground.

Triplett has described the outcrops of the ore bodies and discussed their role in the search for ore. He has pointed out that the conspicuous difference between the productive and the nonproductive outcrops is the relative abundance of iron oxides.

The ore outcrops are marked by deep pits; it is not possible to say whether these are due exclusively to oxidation subsidence or whether surface workings by Spanish miners (as early as the 16th century) contributed to their formation. Samples of the original gossan were obtained from iron oxide remnants found clinging to the walls of these open pits. Long-continued weathering of these oxides has obliterated any definite boxwork structures that may originally have been present.

The gossan material consists of irregular masses and crusts of limonite coated with finely crystalline quartz and rosettes of hemimorphite. Many other metal oxides were identified on surface dumps, but these were not found in place. These minerals have been described by Triplett.

HIDDEN TREASURE MINE, UTAH

Location: Thirty-two miles south of Salt Lake City, Utah; situated between Dry and Ophir Canyons, in the Oquirrh Range.

The lead-zinc ores of the Hidden Treasure mine form extensive pipelike deposits of large dimensions. They follow north-south vertical fissures and are localized within the upper part of the Madison limestone (Mississippian) just below the basal phosphatic shale of the Deseret formation. The ore is roughly parallel to the beds, which strike N. 70°-80° E. and dip 30°-40° N. Many of the old stopes are inaccessible but are said to have been as much as 100 feet high and 50 feet wide, their width depending on the concentration of the controlling north-south fissures (Gilluly, 1932).

Because of the unusual distribution of oxidized and unoxidized ores, this mine is frequently referred to as "the upside-down mine" by local geologists. A major zone of oxidation exists below the primary sulfide zone, far removed from the surface outcrops of the ore. A normal oxide zone overlies the primary unoxidized ore, so that the sulfides are isolated between major oxide zones above and below (fig. 10).

In the lowest present levels of the mine, 1,820 feet below the outcrops on Ophir Hill, the ore intersects a preore rhyolite porphyry dike. Extensive breccias containing both limestone and rhyolite fragments occur along both the eastern and western margins of this dike. In places, these form caves filled with huge angular boulders separated by man-sized openings. These boulders are commonly coated with recrystallized calcite precipitated by descending ground waters. This broken ground has provided a channelway for the descent of oxygen-bearing surface waters and has resulted in the oxidation of ore in proximity to the dike and in the peculiarly deep localization of this part of the oxidation. The lower oxide zone extends from the 500-foot to the 1,150-foot level of the mine, a vertical distance of 650 feet. The upper (normal) oxide zone reaches a depth of 520 feet below the surface outcrops. The isolated sulfide zone has a vertical extent of 650 feet.

The major production has come from the lead and zinc carbonate ores of the mine, although rich sulfide stopes were opened below the present Sovereign (main) tunnel level. The zoning of oxides is such that the lead carbonate ores are sheathed by a thin layer of malachite and azurite which pass outward into a thin but rich shell of zinc carbonate ore. The latter is best developed along the footwall of the ore body. This pattern was described by Gilluly (1932).

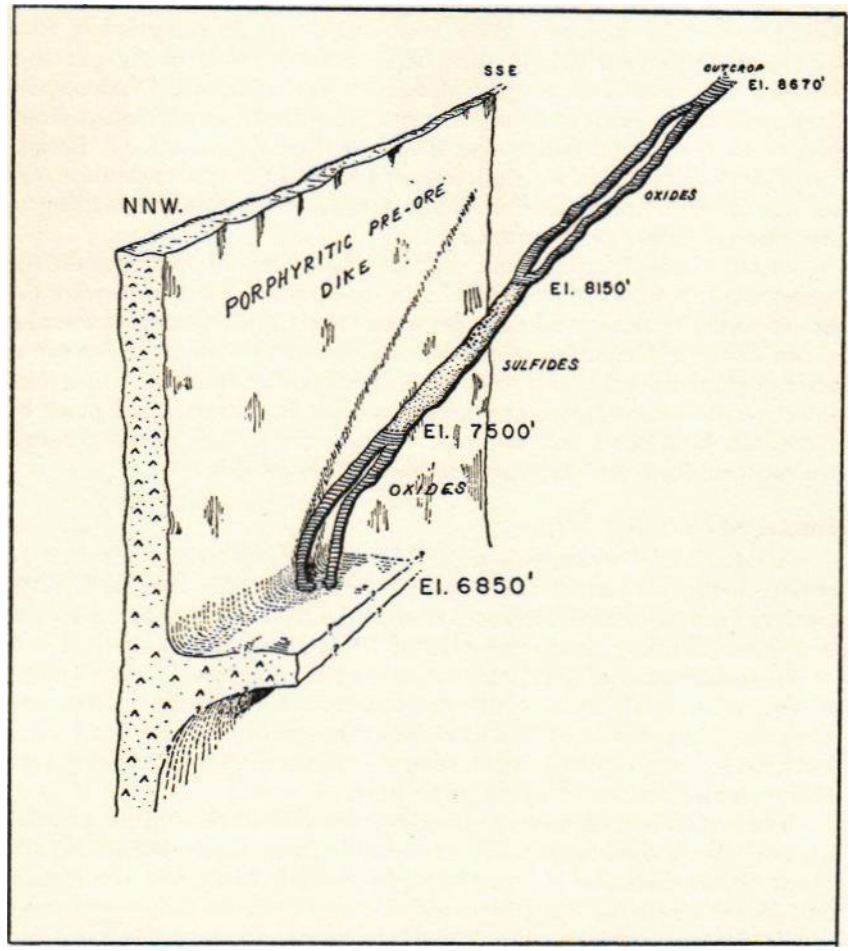

Figure 10

PERSPECTIVE OF THE HIDDEN TREASURE MINE, OPHIR HILL AREA, UTAH

The lead carbonate ore contained an average of 22 percent Pb, 4 to 6 percent Zn, and 18 to 19 oz Ag per ton. The zinc carbonate ores contained 40 percent Zn, 1 percent Cu, and 2 oz Ag per ton. Masses of residual sulfides were mined in the upper oxide zone and are currently being worked in the lower oxide zone. Sulfide ore in the primary zone averaged 30 percent Zn, 14 percent Pb, and 8 to 10 oz Ag per ton. Galena and sphalerite are the dominant ore minerals. Chalcopyrite and pyrite are present and vary in quantity. Gilluly, as previously cited, gives a more comprehensive description of these deposits. G. F. Loughlin (1919) has prepared a detailed description of the zinc carbonate ores and an informative discussion of the processes of oxidation leading to the unusual lamellar structures.

At the time of the writer's visit in 1953, the old workings in the upper oxide zone were inaccessible, but samples of the gossan were obtained at the outcrop of the ore body on Ophir Hill. Samples were also taken in the main sulfide and lower oxide stopes. Limonite boxworks after galena and sphalerite were well developed in both the upper and lower oxide zones. However, the lower zone is characterized more by abundant laminated and botryoidal iron oxides transported through the permeable ground near the rhyolite porphyry dike.

BINGHAM DISTRICT, UTAH

A wealth of literature is available dealing with the disseminated copper deposits of the Utah Copper Stock (especially Boutwell, 1905; Butler, Loughlin, and Heikes, 1920) and the lead-silver-zinc deposits in the surrounding limestones (Hunt, 1924; Hunt and Peacock, 1948).

In the summer of 1952, the writer had an opportunity to examine many, and to study some, of the ore outcrops in this district. Although the principal purpose of this work was the selection of samples for the analytical phases of this project, several features of general interest were observed and are worth mentioning here.

The oxidation of ores in the Bingham district is shallow relative to similar deposits in comparable semiarid climates. Atwood (1916) and Hunt (1924) discussed the recent physiographic history of the district and its effects on the supergene alterations of ore in the copper stock and in the surrounding sediments. Hunt points out that recent erosion has been very rapid and prevented the formation of a thick oxide layer. Unoxidized sulfide ore is actually exposed along beds of the major stream valleys where the rate of erosion has exceeded the rate of oxidation.

Utah Copper Co. Pit

A distinctive pattern of oxidation can be seen in the east and west walls of the Utah Copper Co.'s open pit (fig. 11), where long diagonal bands of oxidized ore extend downward from the surface following the northward dip of the ore-bearing sediments surrounding the quartz

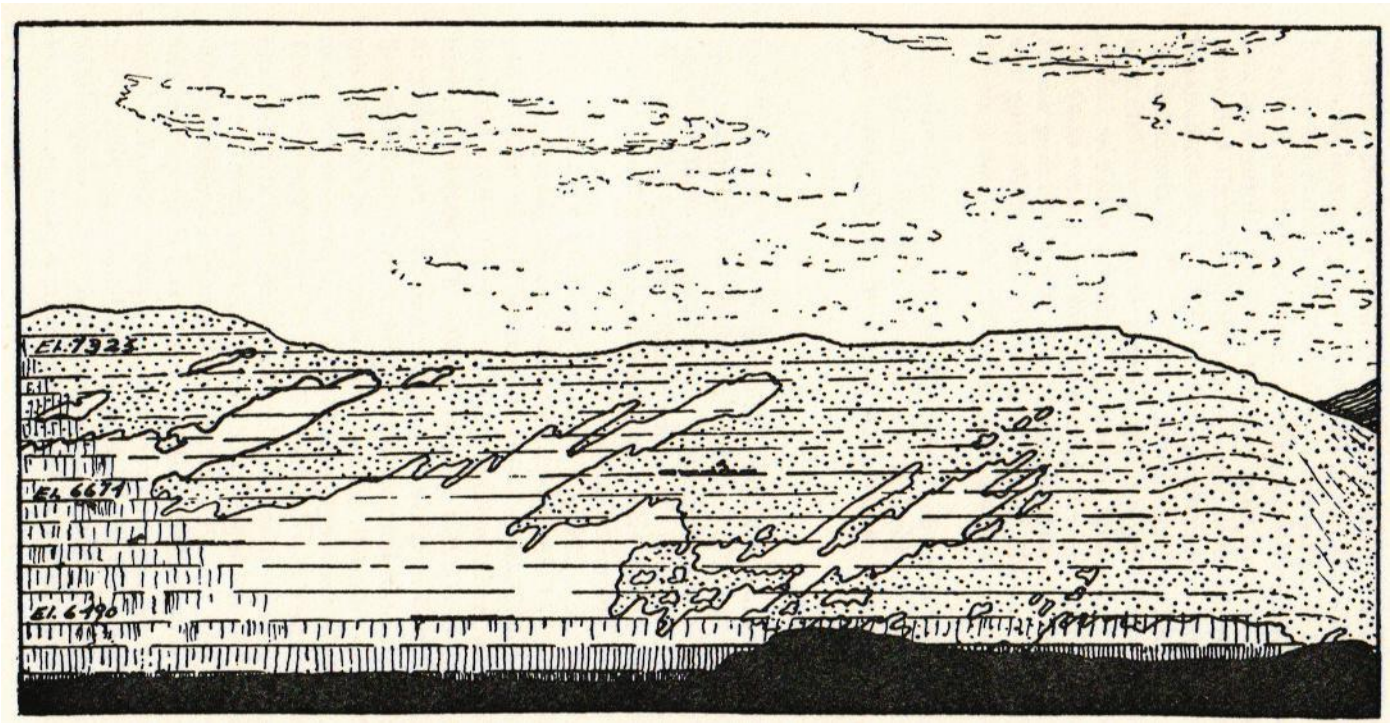

Figure 11

PATTERN OF OXIDATION IN THE UTAH COPPER PIT, BINGHAM, UTAH

A view of the east wall of the copper pit as seen from a west bench, 6,490-foot level, in August 1953. The horizontal lines represent bench levels on the far wall. Mineralized sediments cropping out in this wall have a true exposed dip of about 30° N. Oxidation of the copper ore within these quartzitic strata follows along the bedding and is represented by the stippled areas.

monzonite stock. These sediments consist mainly of Bingham quartzite (Pennsylvanian), which was highly fractured during regional deformation when sediments of the district were folded into a broad northward plunging syncline. Within the quartzite sequence are strata of relatively pure limestone that behaved more plastically during deformation, and which do not display the same degree of shattering (Russell Anderson, Utah Copper Co., personal communication, 1953). These unshattered lime strata have acted as impermeable "shelves" which channeled descending surface water along bedding, thereby confining oxidation to shattered quartzite above, and protecting ore in the quartzite below, for some distance along the beds. Locally the lime strata are more siliceous and have been fractured; in such areas, the descending waters penetrate the impermeable "shelf" and oxidize the underlying ore strata until they encounter another impermeable "shelf" lower in the stratigraphic sequence.

At the south and north ends of the pit, the oxides appear as a shallow layer along the rim of the pit, but here the view is parallel to the dip of the beds, and a true cross-sectional picture of the diagonal oxide pattern is not seen.

Lark Vein

In a search for outcrops whose continuations could be traced into sulfides at depth, most of the lead-zinc deposits of this district were unsuitable, owing to the inaccessibility of the old underground workings. However, at one point along the Lark vein, the workings could be followed down to the sulfide zone along the old Yosemite No. 1 incline at the north fork of Yosemite Gulch.

The Yosemite-Lark workings were developed along a lead-zinc vein which transected both Commercial limestone and Bingham quartzite. In the area studied and sampled, old drifts extended as far as 1,000 feet on either side of the main incline, which is reported to have followed the vein to a depth of 800 feet (Boutwell, 1905). The walls of the vein (average thickness ca. 5 feet) are very regular and show no swelling in passing from quartzite in both walls to limestone in the hanging wall and quartzite in the footwall. Sediments on both sides of the vein dip 30°-39° NW., and the vein itself dips 44 degrees in the same direction.

The ore was oxidized to a depth of 165 feet along the Yosemite No. 1 incline. In the early stages of mining, lead carbonate was extracted from the upper drifts, but the major production has come from the lower stopes in the primary zone. The primary ore contained galena (dominant), sphalerite, and small quantities of pyrite and chalcopyrite. The gangue was composed of country-rock material, quartz, and clay. Some of the lower grade ore left in pillars appeared banded parallel to the vein, with discontinuous but alined patches and streaks of sphalerite and galena embedded in a very friable groundmass of clays. None of

the massive sulfide ores worked from the vein were left in the old workings.

The outcrop of the Lark vein is topographically conspicuous. A prominent ridge is developed along the quartzite footwall of the ore body and locally stands as high as 15 feet above the hillslopes on either side of the vein. Colloidally held or dissolved iron was released on oxidation of sulfides in the vein and gravitated into the footwall, forming limonite along cracks and openings in the shattered quartzite. Apart from their heavy iron staining, the rocks forming the ridges are no different from quartzites elsewhere in the hanging or foot walls. The hanging-wall rocks are unstained and do not form ridges. The prominent footwall ridges are not continuous along the strike of the vein; their discontinuity, however, does not signify a discontinuity of ore but rather an irregular drainage of oxides downward through the footwall.

Much lead carbonate is still present in the outcrop of the vein and occurs (1) as thin layers and coatings on the surface of the footwall, (2) as isolated pockets within the vein and in the footwall close to the vein, and (3) as impregnations of jarosite and limonite that cement fragments of the country rock included in the vein matter. Because of its dull-gray, inconspicuous color in this outcrop, the lead carbonate might easily be passed over on casual inspection, but its presence and distribution were brought out rather spectacularly by a lead iodide spray test described by Jerome (1950).

In general, the structures and distribution of former sulfides in the Lark vein are totally obscured at the outcrop. In rare spots, limonite boxworks after galena and sphalerite were found, but for the most part the iron oxides were not indigenous and occurred as streaks and bands in a pattern which changes from one place to the next. Bands of iron-stained, massive quartz, layers of dense limonite and jarosite, and zones of brecciated quartzite cemented by jarosite and iron oxides paralleled and filled the vein opening at the surface. The bands of massive quartz contained no open voids evidencing the former presence of sulfides and did not continue at depth; they are presumed to be supergene.

EAST TENNESSEE ZINC DISTRICT

The practical value of a gossan study in the more humid regions of this country is, of course, limited, especially if the region is glaciated or has a heavy soil mantle. However, a short time was devoted to study of the oxidation of the zinc deposits of the Jefferson City district of eastern Tennessee, mainly for comparison with oxidized deposits examined in the Southwestern United States. The zinc deposits of east Tennessee have been described by Secrist (1924) and more recently by Brokaw (1948).

A consistent pattern of oxidation was observed in this district which contrasted strongly with conditions in the semiarid Southwest. Figure

12 illustrates this pattern as it is seen in open-pit exposures at the Grasselli and Davis mines, near Jefferson City. Light-green, low-iron (ca. 3 percent) sphalerite is found unoxidized in large pillars of dolomite; between these pillars are pockets or saddles of oxidized ore. Overlying the oxidized ore is a thick (30 to 60 feet) mantle of red acid soil composed mainly of hematite and kaolin. No topographic "slumps" or collapse structures appear over the oxide saddles as clues to the concealment of leached ore. The material contained in the saddles is a mixture of smithsonite, hemimorphite, kaolinite, and minor amounts of iron oxides. The last-named exaggerate their own abundance by staining the admixed clay. The oxidized ore has unusually well-developed box-work structures formed by the removal of zinc sulfide. In places, these boxworks can be traced directly into unoxidized sphalerite. The voids commonly contain coarsely crystalline gypsum formed by interaction of $CaCO_3$ of the gangue and sulfates released on decomposition of the sphalerite.

The development of this pinnacle-saddle structure (terms first used by Secrist, 1924) probably reflects differences in fracturing of the rocks containing the ore. Oxidation has penetrated more deeply into saddle areas, where the rocks are more highly fractured, than in the pinnacles. The saddles were natural channelways for surface solutions migrating downward through the overlying soil mantle and therefore localized the oxidation of ore.

The mine waters of this district have an average pH of 8.0 to 8.2, but the pH of meteoric water percolating through the thick soil mantle onto shallow ore ranges from 5.3 to 6.4.[6] Time has not permitted an investigation of the role of such acid, soil-derived waters in the oxidation of the underlying ores, but it would seem logical that they would tend to accelerate the decomposition of sulfides more than would the waters filtered through more basic soil. The effects of soil mantles were factors of little importance in the districts visited in the semiarid Southwest, but might certainly play an important part in the oxidation of shallow ores in more humid climates.

OTHER SAMPLE SOURCES

The ore deposits of the Elizabeth mine, at Strafford, Vermont, were examined in 1951. These have been most recently, discussed by McKinstry and Mikkola (1954). Pyrrhotite-chalcopyrite ore bodies occur in Paleozoic schists as replacements of a phlogopite-tremolite-carbonate bed in a highly deformed zone of a fold. According to McKinstry and Mikkola, the main ore shoot follows the plunge of an overturned syncline and has a pitch length of 6,000 feet.

The sulfides have been altered to depths of only a few feet; samples of the thin iron capping were taken from open cuts. The gossan con-

6. Data on pH through courtesy of Mr. Edward B. Jennings, Universal Exploration Co., and the Jefferson County Office of the U. S. Dept. of Agriculture.

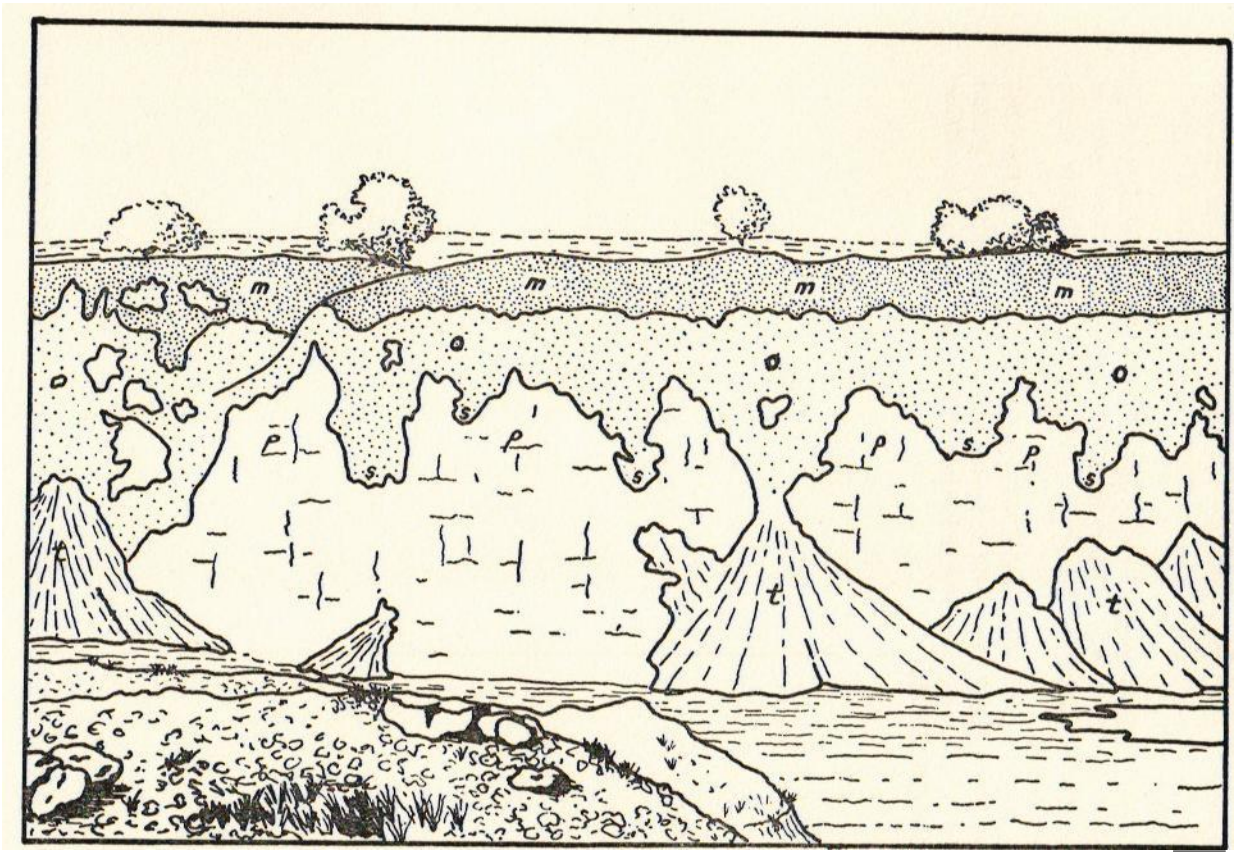

Figure 12

PINNACLE-SADDLE PATTERN OF OXIDATION, GRASSELLI MINE, EAST TENNESSEE

Sketch showing saddles (s) of oxidized ore (o) between pinnacles (p) of unaltered sphalerite in dolomite. The deposits are covered by a thick hematitic soil mantle (m). Talus cones (t) consist mainly of slumped soil material and oxidized ore.

sists mainly of goethite, with intermixed residual flakes of sericite. Very close to the surface, limonite has been precipitated along joints and open spaces in partially oxidized ore. This material showed excellent botryoidal and stalactitic forms and provided fine samples of typical transported limonite.

Many limonite samples were obtained from the economic geology collections at Columbia University, including a complete suite of samples from the cupriferous-pyrite outcrops of the Capote mine, Sonora, Mexico.

Dr. Robert S. Houston, of the department of geology at the University of Wyoming, supplied the writer with a large number of gossan samples from several pyrite-pyrrhotite-chalcopyrite deposits in Maine and New Brunswick.

Appendix B

CONSTRUCTION OF THE Eh-pH DIAGRAM FOR THE SYSTEM Fe—H_2O—CO_2—S AT 25°C

As an example of the procedure followed in obtaining the stability boundaries of Figures 5 and 6, consider the boundary between FeS and FeS_2. Chemically, the change from pyrrhotite to pyrite involves the oxidation of two sulfide ions to form a single polysulfide ion. The reaction may be expressed in the following form:

$$S^{-} FeS = FeS_2\, 2e^{-}. \quad (1)$$

The potential (E°) of this reaction at 25°C, when the sulfide ion has an activity of 1 mole per liter, is related to the free energy of the reaction at unit activity:

$$AF° = — n \cdot 23{,}060 \cdot E°, \quad (2)$$

where n is the number of electrons involved in the reaction, and the constant 23,060 is 1 volt equivalent expressed in units of cal/abs volt gram equivalent.

If the free energies of formation of pyrite, pyrrhotite, and sulfide ion are known, then the free energy of reaction (1) at unit activity may be calculated as the difference between the free energy of formation of pyrite and the sum of the free energies of formation of pyrrhotite and the sulfide ion. The free energies of formation of the dissolved and solid substances which should be considered in this system are known, and the values are listed in Table 5.

$$\begin{aligned} \triangle F° &= \triangle F°_{FeS_2} - \triangle F°_{FeS} - \triangle F°_{S^{--}}, \\ &= -(39{,}840) - (-23{,}320) - (+22{,}100), \\ &= -38{,}620 \text{ calories.} \end{aligned}$$

With this value of AF° , the potential E° of reaction (1) at unit activity may be obtained from equation (2) as follows:

$$\begin{aligned} E° &= -\triangle F°/n \cdot (23{,}060), \\ &= +(38{,}620)/2 \cdot (23{,}060), \\ &= +.837 \text{ volt.} \end{aligned}$$

The oxidation potential at other activities of the sulfide ion may be obtained from the following relationship:

$$E = -E° + \frac{.0591}{u} \log(A_s{}^{--}).$$

TABLE 5. STANDARD FREE ENERGIES OF FORMATION

SOLID SUBSTANCE	$\Delta F°$ (CAL)	SOURCE*
Fe	0	1
FeS	— 23,320	1
FeS_2	— 39,840	1
$Fe(OH)_2$	—115,570	1
$Fe(OH)_3$	—166,000	2
$FeCO_3$	—161,060	1
DISSOLVED SUBSTANCE	**$\Delta F°$ (CAL)**	**SOURCE***
$S--$	+ 22,100	2
SO_4--	—177,340	1
$Fe++$	— 20,300	1
$Fe+++$	— 2,530	1
$FeOH++$	— 55,910	1
FeO_4--	—111,685	3
FeO_2H-	— 90,630	3
H_2CO_3	—149,000	1
HCO_3-	—140,310	1
CO_3--	—126,220	1
H_2O	— 56,690	1
$H+$	0	
$OH-$	— 37,595	1

*1. Listed by Latimer (1953). Original source U. S. Bureau of Standards, Selected values of chemical thermodynamic properties, 1949.
2. Latimer (1953).
3. Deltombe and Pourbaix (1954a, p. 119).

By substitution of the known values of $E°$ and n, this expression becomes:

$$E = -.837 + .0295 \log(A_s--). \quad (3)$$

A substitution may be made here for (A_s--).

It is known that when the pH of a reducing environment is less than 7, the activity of the sulfide ion is controlled by dissociation of H_2S and may be expressed as follows:

$$(A_s--) = (A_{H_2S})(10^{-21})/(A_H+)^2,$$
$$\log(A_s--) = \log(A_{H_2S}) - 21 - 2\log(A_H+).$$

When the pH of the reducing environment is greater than 7, the activity of the sulfide ion is controlled by dissociation of the bisulfide ion. Hence:

$$(A_s--) = (A_{HS}-)(10^{-14})/(A_H+),$$
$$\log(A_s--) = \log(A_{HS}-) - 14 - \log(A_H+).$$

By substitution of these expressions for sulfide-ion activities in equation (3), the following equations are obtained:

$$E = -.837 + .0295\,[\log(A_{H_2S}) - 21 - 21\log(A_{H^+})], \quad \text{where pH} < 7;$$
$$E = -.837 + .0295\,[\log(A_{HS^-}) - 14 - \log(A_{H^+})], \quad \text{where pH} > 7.$$

Finally, these equilibrium formulae may be reduced to a simplified form:

$$E = -.217 - .0295\log(A_{H_2S}) - .0591\,\text{pH}, \quad \text{where pH} < 7;$$
$$E = -.424 - .0295\log(A_{HS^-}) - .0295\,\text{pH}, \quad \text{where pH} > 7.$$

Points on the equilibrium boundary between pyrrhotite and pyrite may be readily calculated from these last two equations by assigning a pH value and solving for *E* in the appropriate equation. In a reducing environment such as that which would prevail along the pyrite-pyrrhotite boundary, the assumed value of total dissolved sulfur may be substituted for either AH2S or AHS—.

A similar procedure was followed in obtaining all other boundary curves in the equilibrium diagram.

Where H_2CO_3, HCO_3—, or CO_3^{--} was involved in a reaction, it was necessary to calculate the activity of the involved ion for substitution in the equilibrium formulae at a selected pH. Because many such activities were needed in construction of the diagram, the writer calculated, as a first step, the values of the activity of H_2CO_3, HCO_3—, and CO_3^{--} for all integral values of pH from 1 to 14 at assumed total dissolved-CO_2 concentrations of 10^0, 10^{-1}, 10^{-2}, 10^{-3}, 10^{-4}, 10^{-5}, and 10^{-6} mole per liter. These activities were calculated from the following relationships:

$$\lessgtr \text{dissolved } CO_2 = \lessgtr (A_{H_2CO_3} + A_{HCO_3^-} + A_{CO_3^{--}}) = \text{some assumed molarity},$$
$$\frac{A_{H^+} \cdot A_{HCO_3^-}}{A_{H_2CO_3}} = 10^{-6.4},$$
$$\frac{A_{H^+} \cdot A_{CO_3^{--}}}{A_{HCO_3^-}} = 10^{-10.5}.$$

With these data at hand, it was a relatively simple matter to calculate change in siderite boundaries with variations in total dissolved CO2.

Appendix C

METHOD USED FOR THE DETERMINATION OF THE POROSITY VALUES (PRIMARY-ORE SAMPLES) LISTED IN TABLE 3

The procedure followed for determining gossan porosities could not be used for the primary-ore samples because the porosities of the ores were low and their pores small and poorly connected.

The pycnometer was not used in any of these porosity determinations. Although fairly accurate, the specific-gravity bottle (even the wide-mouthed variety) cannot accommodate a large, wax-coated sample.

Step 1. Weigh the sample in air (W_1).

Step 2. Coat the sample with wax and weigh in air (W_2).

This is best accomplished by melting paraffin in a pyrex beaker. The cold sample is quickly dipped into the wax for a thin overall coating. A small medicine dropper kept hot by leaving it in the beaker with the wax can then be used to drop hot paraffin onto those spots where the first coating did not provide a perfect seal.

Step 3. Weigh the coated sample in distilled water (W_e).

Step 4. Dissolve the wax coating in benzene or another suitable solvent, and reweigh the sample (W_1').

It is important that (WO equal (W_1). If the check weighing is greater than the original weighing, then the coating has not been completely dissolved, or the sample has not been given a proper chance to dry. If the check is less than the original weighing, then some material has been lost from the sample, and the procedure must be repeated from the start.

Step 5. Determine bulk volume of sample by displacement of alcohol in a narrow graduated pipette (V).

The sample is ground to about 40 mesh in a clean iron mortar. It is then poured slowly into a narrow graduated pipette (calibrated to 0.1 cc) containing a known quantity of ethyl alcohol. Other liquids of low surface tension are just as suitable. The pipette must be shaken until all air lodged between the sample particles is freed. The level of the alcohol will reach a constant point, beyond which further shaking causes no change. The displaced volume of alcohol is the bulk volume of the sample.

1. If K = specific volume of the paraffin, then the buoyant force on the sample in W3 due to the wax coating (if the measurement is made in metric units) is (K — 1) (W_2 — W_1).
2. Volume bulk plus voids is equal to W_1 — W3 +K — 1) (W2 — W1).

3. Sample volume bulk = V.
4. Percent porosity = volume voids/volume bulk + voids X 100:

$$\frac{W1 - W3 + (K - 1)(W2 - W1 - V}{W1 - W2 + (K-1)(W2 - W1)}$$

The specific volume of the paraffin is best determined by using a pycnometer.

Appendix D

CALCULATION OF VOLUMETRIC PERCENTAGES OF SULFIDES IN SHINGLE CANYON ORE SAMPLES FROM ASSAY RETURNS

Assumption: Since pyrite was negligible in the ore, it was assumed that all reported Fe was combined as FeS in marmatite. Known quantities needed in calculations:

Atomic weight Zn	65.38
Atomic weight Fe	55.84
Atomic weight S	32.06
Zn assay (wt.% Zn)	19.4
Fe assay (wt.% Fe)	8.3
Density ore	3.24(measured)
Density ZnS	4.00(assumed)
Density FeS	4.61(assumed)

Step 1. Calculation of weight percent ZnS and weight percent FeS in ore:

$$\text{Wt. \% ZnS} = \text{wt. \% Zn} + \text{wt. \% S},$$
$$= 19.4 + \frac{\text{at. wt. S}}{\text{at. wt. Zn}} \times 19.4;$$
$$\text{Wt. \% ZnS} = 28.6\%;$$
$$\text{Wt. \% FeS} = 13.1\% \text{ (following the same procedure).}$$

Step 2. Calculation of volumetric percentages of ZnS and FeS frQm their weight percentages:

$$\text{Vol. \% ZnS} = \text{vol. ZnS}/\text{vol. ore} \times 100,$$
$$\text{and since vol. ZnS} = \text{wt. ZnS}/\text{density ZnS},$$
$$\text{and vol. ore} = \text{wt. ore}/\text{density ore},$$

by substitution,

$$\text{Vol. \% ZnS} = \frac{\text{wt. ZnS}/\text{density ZnS}}{\text{wt. ore}/\text{density ore}} \times 100,$$
$$= \frac{\text{density ore} \times \text{wt. ZnS}}{\text{density ZnS} \times \text{wt. ore}} \times 100,$$
$$= \frac{\text{density ore} \times \text{wt. \% ZnS}}{\text{density ZnS}} \times 100.$$
$$\text{Vol. \% ZnS} = 23.2$$
$$\text{Vol. \% FeS} = 9.2 \text{ (following the same procedure)}$$
$$\text{Total vol. \% marmatite} = 32.4$$

Appendix E

X-RAY DIFFRACTION DATA ON GOSSAN GOETHITES

Powder patterns listed were obtained by the Ievins-Straumanis (asymmetric) method. Fe radiation. Mn filter. Two hours exposure. 40-kv working potential. d-values are listed in Angstrom units. Intensities were estimated visually.

Sample 1

Standard pattern. Goethite (impure) (Smitheringale, 1929, p. 494). ASTM card no. 2-0281.

d(Å)	I visual	d(Å)	I visual	d(Å)	I visual
4.50	50	1.72	100	1.20	50
4.08	100	1.68	50	1.16	20
3.34	50	1.65	20	1.15	50
2.93	50	1.60	50	1.14	50
2.66	100	1.56	90	1.13	70
2.55	50	1.51	70	1.10	50
2.43	100	1.47	20	1.07	50
2.24	70	1.42	50	1.06	60
2.17	90	1.39	50	1.04	20
2.00	20	1.37	50	1.03	50
1.92	50	1.36	50	1.02	90
1.89	50	1.32	70	1.01	70
1.79	50	1.29	20		
1.77	20	1.24	50		

Sample 2

Standard pattern. Goethite (Harcourt, 1942, p. 84). ASTM card no. 3-0251.

d(Å)	I visual	d(Å)	I visual	d(Å)	I visual
4.17	100	1.73	30	1.14	5
3.36	5	1.58	5	1.12	5
2.69	20	1.57	10	1.05	5
2.46	40	1.51	10	1.02	5
2.21	20	1.46	10	1.01	5
1.92	5	1.31	5		
1.80	10	1.20	5		

Sample 3

Standard pattern. Goethite (Harcourt, 1942, p. 84). ASTM card no. 2-0402.

d(Å)	I visual	d(Å)	I visual	d(Å)	I visual
4.98	4	2.19	20	1.56	28
4.21	100	1.92	8	1.50	24
3.39	12	1.80	8	1.46	12
2.70	36	1.72	36	1.42	4
2.58	24	1.68	4	1.36	8
2.45	80	1.65	4	1.32	12
2.25	12	1.60	8		

Sample 4

Standard pattern. Goethite (Peacock, 1942, p. 116). ASTM card no. 2-0272.

d(Å)	I visual	d(Å)	I visual	d(Å)	I visual
5.00	20	2.09	5	1.47	40

4.60	40	2.00	10	1.42	20
4.18	100	1.91	20	1.39	20
3.36	30	1.80	40	1.36	30
2.98	20	1.77	5	1.34	5
2.69	80	1.72	70	1.32	30
2.57	20	1.68	30	1.29	20
2.47	20	1.66	20	1.27	20
2.45	80	1.60	30	1.26	10
2.25	30	1.56	50		
2.18	50	1.51	40		

Sample 5

Standard pattern. Goethite (Second Chelchom mine, Middle Ural). ASTM card no. 2-0273.

d(Å)	I visual	d(Å)	I visual	d(Å)	I visual
4.18	100	2.19	60	1.56	60
3.39	30	1.92	10	1.51	40
2.69	80	1.83	20	1.42	20
2.58	30	1.72	80	1.40	20
2.45	100	1.69	20	1.36	10
2.25	40	1.60	20	1.32	20

Sample 6

Goethite pseudomorph after pyrite (Slane County, Texas).

d(Å)	I visual	d(Å)	I visual	d(Å)	I visual
4.60	35	2.41	5	1.77	Indistinct
4.18	100	2.30	4	1.72	70
3.74	Indistinct	2.25	20	1.69	10
3.34	5	2.19	50	1.66	5
2.97	10	2.09	Indistinct	1.60	10
2.69	80	2.01	2	1.56	50
2.59	20	1.99	2	1.51	10
2.53	3	1.92	5	1.46	Indistinct
2.49	25	1.89	5	1.42	Indistinct
2.45	80	1.80	10		

Sample 7

Goethite pseudomorph after pyrite (Llano, Texas).

d(Å)	I visual	d(Å)	I visual	d(Å)	I visual
4.97	20	2.45	80	1.77	3
4.61	20	2.42	Indistinct	1.72	50
4.17	100	2.30	Indistinct	1.69	20
3.72	Indistinct	2.25	30	1.66	5
3.38	20	2.19	40	1.60	15
2.97	10	2.09	Indistinct	1.56	40
2.85	Indistinct	2.01	Indistinct	1.51	20
2.69	80	1.98	Indistinct	1.46	Indistinct
2.58	30	1.92	5	1.42	5
2.52	3	1.89	5		
2.48	30	1.80	15		

Sample 8

Goethite from gossan of pyritic lead-zinc ore (Providencia mine, Zacatecas, Mexico).

d(Å)	I visual	d(Å)	I visual	d(Å)	I visual
5.01	5	2.50	Indistinct	1.72	20
4.70	3	2.46	80	1.69	Indistinct

4.64	3	2.29	Indistinct	1.61	Indistinct
4.29	20	2.25	Indistinct	1.57	10
4.19	90	2.20	15	1.55	10
3.71	20	2.13	10	1.52	15
3.35	100	2.01	Indistinct	1.46	5
2.71	80	1.98	5		
2.59	10	1.82	20		

Sample 9

Goethite from gossan of pyritic lead-zinc ore (Providencia mine, Zacatecas, Mexico).

d(Å)	I visual	d(Å)	I visual	d(Å)	I visual
6.56	5	2.60	20	1.73	50
5.01	10	2.50	Indistinct	1.70	10
4.63	10	2.46	80	1.61	10
4.20	100	2.41	Indistinct	1.57	30
3.71	8	2.26	10	1.51	30
3.36	50	2.20	20	1.46	30
3.11	3	2.01	Indistinct	1.41	5
2.98	3	1.93	3		
2.71	80	1.81	5		

Sample 10

Goethite from gossan of pyritic lead-zinc ore (Providencia mine, Zacatecas, Mexico).

d(Å)	I visual	d(Å)	I visual	d(Å)	I visual
4.97	20	2.60	20	1.72	50
4.60	20	2.49	10	1.69	5
4.18	100	2.45	80	1.66	3
3.38	10	2.25	20	1.60	10
3.29	Indistinct	2.19	40	1.57	30
3.09	Indistinct	1.93	Indistinct	1.51	15
3.02	10	1.89	Indistinct	1.46	10
2.70	80	1.80	10		

Sample 11

Goethite from gossan of lead-zinc ore (Hidden Treasure mine, Utah).

d(Å)	I visual	d(Å)	I visual	d(Å)	I visual
5.01	20	2.49	5	1.66	3
4.63	20	2.45	80	1.61	5
4.19	100	2.26	25	1.57	40
3.36	10	2.19	25	1.51	20
2.98	5	1.93	Indistinct	1.46	10
2.70	80	1.80	5	1.42	3
2.59	30	1.72	50		
2.53	Indistinct	1.69	5		

Sample 12

Goethite pseudomorph after pyrite (Ashboro, North Carolina).

d(Å)	I visual	d(Å)	I visual	d(Å)	I visual
5.00	10	2.58	10	1.70	5
4.62	10	2.52	5	1.61	Indistinct
4.18	100	2.45	80	1.56	20
3.35	5	2.25	20	1.51	15
2.99	Indistinct	2.19	30		
2.69	80	1.72	50		

Sample 13

Goethite from pyrite gossan (Capote mine, Sonora, Mexico).

d(Å)	I visual	d(Å)	I visual	d(Å)	I visual
4.99	Indistinct	2.59	20	1.72	25
4.66	Indistinct	2.45	80	1.57	25
4.21	100	2.25	5	1.53	25
3.69	20	2.20	10	1.42	2
3.35	90	2.13	Indistinct		
2.70	80	1.82	10		

Sample 14

Goethite from gossan of lead-zinc ore (Lark vein, Bingham, Utah).

d(Å)	I visual	d(Å)	I visual	d(Å)	I visual
4.98	5	2.70	80	1.72	65
4.62	15	2.59	10	1.56	50
4.20	100	2.49	Indistinct	1.51	40
3.35	Indistinct	2.45	80	1.46	Indistinct
3.07	10	2.26	10		
2.97	Indistinct	2.20	8		

Sample 15

Goethite from pyrite gossan (Pewabic mine, Hanover, New Mexico).

d(Å)	I visual	d(Å)	I visual	d(Å)	I visual
4.98	10	2.45	80	1.69	Indistinct
4.64	10	2.26	15	1.57	50
4.19	100	2.19	20	1.51	35
2.70	80	1.80	Indistinct	1.46	10
2.59	8	1.72	70		

Sample 16

Goethite from pyrite gossan (Milan mine, New Hampshire).

d(Å)	I visual	d(Å)	I visual	d(Å)	I visual
4.97	Indistinct	2.44	80	1.63	10
4.60	Indistinct	2.25	10	1.56	15
4.18	100	2.20	10	1.51	10
2.70	80	1.92	5		
2.59	20	1.72	5		

Sample 17

Goethite from gossan of lead-zinc ore (Lordsburg, New Mexico).

d(Å)	I visual	d(Å)	I visual	d(Å)	I visual
4.66	10	2.70	70	1.82	10
4.23	80	2.60	Indistinct	1.57	Indistinct
3.68	20	2.46	70	1.54	Indistinct
3.34	100	2.28	Indistinct		
2.98	Indistinct	2.13	Indistinct		

Sample 18

Goethite from gossan of zinc ore (Grant County, New Mexico).

d(Å)	I visual	d(Å)	I visual	d(Å)	I visual
4.93	Indistinct	2.58	10	1.69	40
4.60	10	2.45	80	1.55	20
4.18	100	2.25	5	1.51	20
2.70	80	2.19	5		

Sample 19

Transported (laminated) goethite derived from pyrite (New Mayberry mine, Bingham, Utah).

d(Å)	I visual	d(Å)	I visual	d(Å)	I visual
4.20	80	2.45	80	1.54	10
3.34	100	2.25	10	1.51	4
2.69	30	1.82	10	1.38	20
2.55	Indistinct	1.73	5		

Sample 20

Transported (fluffy type) goethite derived from pyrite (New Mayberry mine, Bingham, Utah).

d(Å)	I visual	d(Å)	I visual	d(Å)	I visual
4.22	100	2.27	20	1.57	5
3.33	80	1.82	20	1.51	5
2.69	10	1.73	10	1.37	5
2.45	80	1.71	15		

Sample 21

Goethite from gossan of zinc ore (Pewabic quarry, Hanover, New Mexico).

d(Å)	I visual	d(Å)	I visual	d(Å)	I visual
4.63	5	2.58	Indistinct	1.56	Indistinct
4.22	100	2.52	5	1.51	50
3.34	10	2.45	90		
2.70	80	1.72	50		

Sample 22

Goethite from gossan of zinc ore (Grant County, New Mexico).

d(Å)	I visual	d(Å)	I visual	d(Å)	I visual
4.19	80	3.13	Indistinct	2.52	80
3.67	10	2.96	10	2.44	80
3.34	100	2.70	80	1.60	Indistinct

Sample 23

Transported goethite (stalactitic) derived from lead-zinc ores (Hidden Treasure mine, Utah).

d(Å)	I visual	d(Å)	I visual	d(Å)	I visual
4.21	100	2.58	30	1.80	10
3.35	40	2.45	90	1.72	20
2.70	80	2.25	10	1.57	10

Sample 24

Goethite from pyrite gossan (New Mayberry mine, Bingham, Utah).

d(Å)	I visual	d(Å)	I visual	d(Å)	I visual
4.20	100	2.46	90	1.73	10
2.69	80	2.25	5	1.56	10
2.59	20	2.18	7	1.51	10

Sample 25

Goethite from gossan of pyrite-chalcopyrite-pyrrhotite ore (Strafford mine, Vermont).

d(Å)	I visual	d(Å)	I visual	d(Å)	I visual
4.20	100	2.45	80	1.72	50
2.70	80	2.25	5	1.57	30
2.58	10	2.19	5	1.51	10

Sample 26

Goethite from gossan of zinc ore (Bullfrog mine, Vanadium, New Mexico).

d(Å)	I visual	d(Å)	I visual	d(Å)	I visual
4.18	100	2.59	30	1.57	20
3.34	70	2.45	90	1.51	10
2.69	80	1.72	50		

Sample 27

Goethite pseudomorph after pyrite (locality unknown).

d(Å)	I visual	d(Å)	I visual	d(Å)	I visual
4.19	100	2.59	20	1.72	10
3.34	80	2.45	90	1.57	8
2.70	90	2.25	5		

Sample 28

Goethite from pyrite gossan (Bullfrog mine, Vanadium, New Mexico).

d(Å)	I visual	d(Å)	I visual	d(Å)	I visual
7.68	Indistinct	3.34	100	1.72	30
4.20	90	2.70	80		
3.68	10	2.45	80		

Sample 29

Goethite forming boxworks in partially weathered magnetite (Pewabic quarry, Hanover, New Mexico).

d(Å)	I visual	d(Å)	I visual
4.19	100	2.45	70
3.33	80	1.72	30
2.70	70		

Sample 30

Goethite from gossan of zinc ore (Shingle Canyon, New Mexico).

d(Å)	I visual	d(Å)	I visual
4.20	100	2.70	80
3.33	20	2.45	80

References

Almond, Hy, and Morris, H. T. (1951) *Geochemical techniques as applied in recent investigations in the Tintac district, Utah,* Econ. Geol., v. 46, p. 608-625.

Anderson, C. A. (1950) *Alteration and metallization in the Bagdad porphyry copper deposit, Arizona,* Econ. Geol., v. 45, p. 609-628.

Atwood, W. W. (1916) *The physiographic conditions at Butte, Montana, and Bingham Canyon, Utah, when the copper ores in these districts were enriched,* Econ. Geol., v. 11, p. 697-740.

Bateman, A. M. (1950) *Economic mineral deposits,* New York, John Wiley & Sons, p. 258-259.

Blanchard, Roland (1939a) *Interpretation of leached outcrops,* Chem. Metall. Mining Soc. South Africa Jour., p. 16-25.

——— (1939b) *Significance of the iron oxide outcrop at Mount Oxide, Queensland,* Australasian Inst. Min. Met. Proc., new ser., n. 114, p. 21-54.

——— (1942) *Leached derivatives of arsenopyrite and chromite,* Econ. Geol., v. 37, p. 596-626.

——— (1944) *Chemical and mineralogical composition of twenty typical "limonites,"* Amer. Min., v. 29, p. 111-114.

———, and Boswell, P. F. (1925) *Notes on the oxidation products derived from chalcopyrite,* Econ. Geol., v. 20, p. 613-641.

———, and ——— (1930) *Limonite types derived from bornite and tetrahedrite,* Econ. Geol., v. 25, p. 557-580.

———, and ——— (1934) *Additional limonite types of galena and sphalerite derivation,* Econ. Geol., v. 29, p. 671-690.

Boswell, P. F., and Blanchard, Roland (1927) *Oxidation products derived from sphalerite and galena,* Econ. Geol., v. 22, p. 419-453.

———, and ——— (1929) *Cellular structure in limonite,* Econ. Geol., v. 24, p. 791-796.

Boutwell, J. M. (1905) *Economic geology of the Bingham mining district,* U. S. Geol. Survey Prof. Pap. 38.

Bragg, W. H. (1937) *Atomic structure of minerals,* Ithaca, Cornell University Press, p. 111-113.

Brindley, G. W., et al. (1951) *X-ray identification and crystal structures of clay minerals,* London, Taylor and Francis, Ltd., p. 260-261.

Brokaw, A. L. (1948) *Geology and mineralogy of the East Tennessee zinc district,* Int. Geol. Cong., 18th, Proc., pt. 7, Pb-Zn symposium, p. 70-76.

Butler, B. S., et al. (1920) *The ore deposits of Utah,* U. S. Geol. Survey Prof. Pap. 111, p. 340-362.

Callaghan, Eugene (1938) *Metalliferous mineral deposits of the Cascade Range in Oregon,* U. S. Geol. Survey Bull. 893, p. 33.

Chayes, Felix (1949) *A simple point counter for thin-section analysis,* Amer. Min., v. 34, p. 1-11.

Deltombe, E., and Pourbaix, M. (1954a) *Equilibrium potential-pH diagrams for iron at 25°C.,* Int. Comm. Electrochemical Thermodynamics and Kinetics, 6th Meeting, Proc., p. 118-123.

———, and ——— (1954b) *Equilibrium potential-pH diagram for the system Fe-CO_2-H_2O at 25°C,* Int. Comm. Electrochemical Thermodynamics and Kinetics, 6th Meeting, Proc., p. 124-132.

Emmons, W. H. (1910) *The Milan mine, New Hampshire,* U. S. Geol. Survey Bull. 432, p. 50-60.

Federico, Marcella, and Fornaseri, Mario (1953) *Fenomeni di trasformazione dei pirosseni de giacimenti ferriferi dell' Isola d'Elba,* Periodico Mineralogia, an. 22, n. 1, p. 107-127.

Gheith, M. A. (1953) *Stability relations of ferric oxides and their hydrates,* Int. Geol. Congress, 19th, sec. 10, fasc. 10, p. 79-80.

Gilluly, James (1932) *Geology and ore deposits of the Stockton and Fairfield quadrangles, Utah,* U. S. Geol. Survey Prof. Pap. 173, p. 144-146.

Goddard, E. N. (editor) (1948) *Rock color chart,* Rock Color Chart Committee, National Research Council, Washington, Superintendent of Documents.

Goldsztaub, M. S. (1935) *Études de quelques dérivés de l'oxyde ferrique (FeO · OH, FeO_2Na, FeO · Cl); détermination de leurs structures,* Soc. franç. minéralogie Bull. 58, p. 17-24.

Harcourt, G. A. (1942) *Tables for the identification of ore minerals by X-ray powder patterns,* Amer. Min., v. 27, p. 84.

Henry, N. F. M., Lipson, H., and Wooster, W. A. (1951) *The interpretation of X-ray diffraction photographs,* London, Macmillan & Co., p. 213-218.

Hewett, G. F. (1931) *Geology and ore deposits of the Goodsprings quadrangle, Nevada,* U. S. Geol. Survey Prof. Pap. 162, p. 112-113.

Holmes, Arthur (1930) *Petrographic methods and calculations,* 2d ed., London, Thos. Murby, p. 313-319.

Hunt, R. N. (1924) *The ores in the limestones at Bingham, Utah,* Amer. Inst. Min. Met. Eng. Trans., v. 70, p. 856-883.

———, and Peacock, H. G. (1948) *Lead and lead-zinc ores of the Bingham district, Utah,* Int. Geol. Cong., 18th, Proc., pt. 7, Pb-Zn symposium, p. 92-96.

Jerome, S. E. (1950) *Special field applications of a confirmatory test for lead,* Econ. Geol., v. 45, p. 358-362.

Kerr, P. F., and Kulp, J. L. (1948) *Multiple differential thermal analysis,* Amer. Min., v. 33, p. 387-419.

Krauskopf, K. B. (1957) *Separation of manganese from iron in sedimentary processes,* Geochim. et Cosmochim. Acta, v. 12, 61-84.

Krumbein, W. C., and Garrels, R. M. (1952) *Origin and classification of chemical sediments in terms of pH and oxidation-reduction potentials,* Jour. Geol., v. 60, p. 1-33.

Kulp, J. L. and Adler, H. H. (1950) *Thermal study of jarosite,* Am. Jour. Sci., v. 248, p. 475-487.

———, and Kerr, P. F. (1949) *Improved multiple differential thermal analysis apparatus,* Amer. Min., v. 34, p. 839-845.

———, and Trites, A. F. (1951) *Differential thermal analysis of the natural hydrous ferric oxides,* Amer. Min., v. 36, p. 23-44.

Larsen, E. S., and Miller, F. S. (1935) *The Rosiwal method and modal determination of rocks,* Amer. Min., v. 20, p. 260-273.

Lasky, S. G. (1936) *Geology and ore deposits of the Bayard Area, Central mining district, New Mexico,* U. S. Geol. Survey Bull. 870, p. 121-124.

——— (1938) *Geology and ore deposits of the Lordsburg mining district, Hidalgo County, New Mexico,* U. S. Geol. Survey Bull. 885.

———, and Hoagland, A. D. (1948) *Central mining district, New Mexico,* Int. Geol. Cong., 18th, Proc., pt. 7, Pb-Zn symposium, p. 97-110.

Latimer, W. M. (1953) *The oxidation states of the elements and their potentials in aqueous solution,* 2d ed., New York, Prentice-Hall, Inc.

Locke, Augustus (1926) *Leached outcrops as guides to copper ore,* Baltimore, Williams and Wilkins.

Loughlin, G. F. (1919) *Zinc carbonate and related copper carbonate ores at Ophir, Utah,* U. S. Geol. Survey Bull. 690, p. 1-14.

McKinstry, H. E., and Mikkola, A. A. (1954) *The Elizabeth copper mine, Vermont,* Econ. Geol., v. 49, p. 1-30.

Merwin, H. E. (1913) *Media of high refraction for refractive index determinations with the microscope; also a set of permanent standard media of lower refraction,* Washington Acad. Sci. Jour., v. 3, p. 35-40.

———, and Larsen, E. S. (1912) *Mixtures of amorphous sulphur and selenium for the determination of high refractive indices with the microscope,* Amer. Jour. Sci., v. 34, p. 42-47.

Nishihara, G. S. (1914) *The rate of reduction of acidity of descending waters and its bearing on secondary sulfide enrichment,* Econ. Geol., v. 9, p. 743-757.

Paige, Sidney (1909) *The Hanover iron-ore deposits,* U. S. Geol. Survey Bull. 380, p. 199-214.

Peacock, M. A. (1942) *On goethite and lepidocrocite,* Roy. Soc. Canada Trans., v. 36, iv, p. 116.

Posnjak, E., and Merwin, H. E. (1919) *The hydrated ferric oxides,* Amer. Jour. Sci., v. 47, p. 311-348.

———, and ——— (1922) *The system Fe_2O_3-SO_3-H_2O,* Amer. Chem. Soc. Jour., v. 44, p. 1965-1993.

Sandell, E. B. (1950) *Colorimetric determination of traces of metals,* 2d ed., New York, Interscience Publishers.

Schmitt, Harrison (1939a) *Outcrops of ore shoots,* Econ. Geol., v. 34, p. 654-673.

——— (1939b) *The Pewabic mine,* Geol. Soc. Am. Bull., v. 50, p. 777-818.

Secrist, M. H. (1924) *Zinc deposits of east Tennessee,* Tennessee Div. Geol. Bull., v. 31.

Short, M. N. (1940) *Microscopic determination of the ore minerals,* U. S. Geol. Survey Bull. 914, p. 187-190.

Smitheringale, W. V. (1929) *Notes on etching tests and X-ray examination of some manganese minerals,* Econ. Geol., v. 24, p. 494.

Spiel, S., et al. (1945) *Differential thermal analysis. Its application to clays and other aluminous minerals,* U. S. Bur. Mines Tech. Pap. 664.

Triplett, W. H. (1952) *Geology of the silver-lead-zinc deposits of the Avalos-Providencia district of Mexico,* Mining Eng., v. 4, p. 582-593.

Trischka, C., Rove, O. N., and Barringer, D. M., Jr. (1929) *Boxwork siderite,* Econ. Geol., v. 24, p. 677-689.

Trites, A. F. (1948) *Differential thermal analysis of goethite and lepidocrocite* (unpublished), Columbia Univ. Master's thesis.

Tunell, George (1930) *The oxidation of disseminated copper ores in altered porphyry* (unpublished), Harvard Univ. Doctoral dissertation.

Weiser, H. B. (1926) *The hydrous oxides,* New York, McGraw-Hill Book Co., Inc., p. 70-74.

———, and Milligan, W. O. (1935) *X-ray studies of the hydrous oxides,* Jour. Phys. Chem., v. 39, p. 25-34.

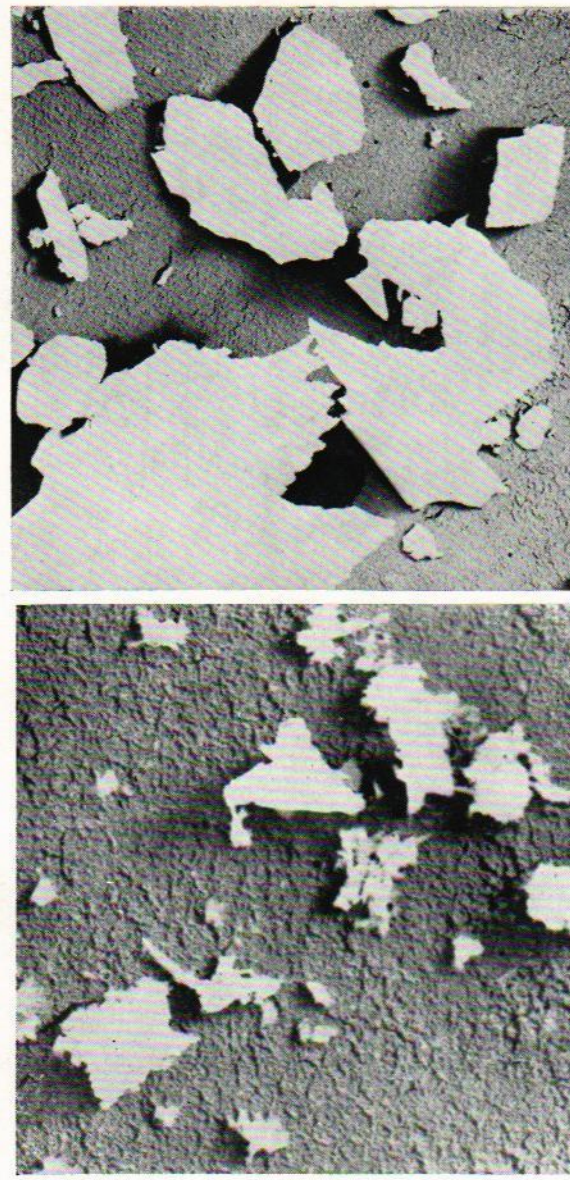

Plate 1

ELECTRON PHOTOMICROGRAPHS OF GOETHITE

A. Well-crystallized goethite, Tavistock, Devonshire. This material decomposes at 400°C, producing a standard thermal curve for goethite. Note the consolidated appearance of the particles and their sharp crystalline edges. Scale × 9,600.

B. Poorly crystallized goethite from gossan at Hidden Treasure mine, Utah. This material decomposes at about 340°C. Some elongated forms can be seen; these may be crystallites. In general, the gossan goethites appear as clotted aggregates of limonite, with evidence of incipient crystallization only in a few particles. Scale × 9,600.

Plate 2

LIMONITE BOXWORKS

A. Limonite boxwork after limestone, Copperside mine, Goodsprings, Nevada. Scale × ½.
B. Limonite boxworks after limestone, New Mayberry mine, Bingham, Utah. Scale × 1.

A

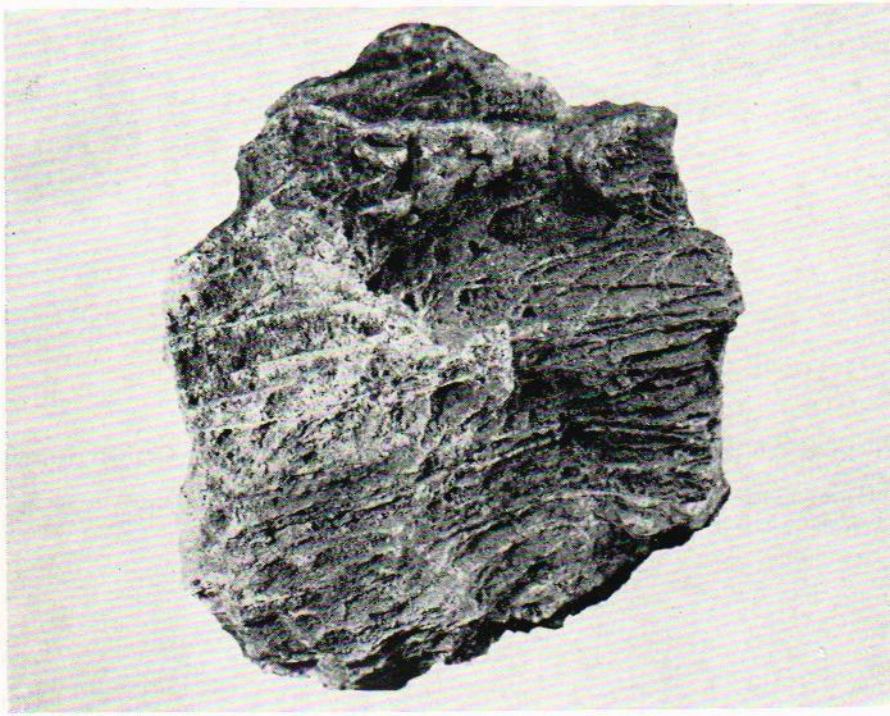

B

Plate 3

LIMONITE AND SMITHSONITE STRUCTURES

A. Limonite boxwork after limestone, Hidden Treasure mine, Ophir Hill area, Utah. Scale × ¾.

B. Layered smithsonite after limestone, Hidden Treasure mine, Ophir Hill area, Utah. The shape of the ridges and of the intervening open spaces was controlled by the pattern of fractures in the original limestone and by variations in the permeability of the replaced rock. Scale × ½.

A

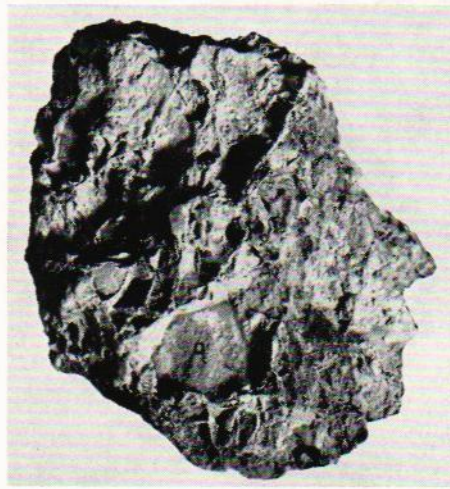

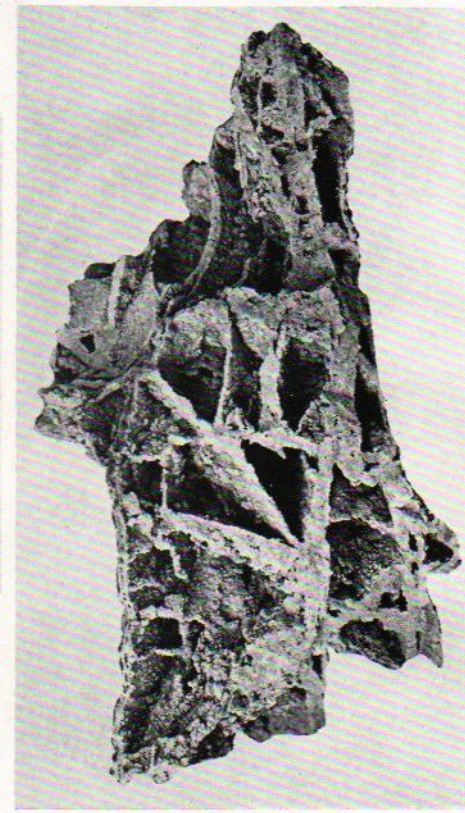

B

Plate 4

BOXWORKS

A. Boxwork of hypogene silica after quartzite, Lark vein, Utah. Fragments of unleached quartzite (q) in some of the cavities in this specimen. Scale × 1¼.

B. Boxwork siderite after limestone, Bisbee, Arizona (by G. F. Loughlin; courtesy of the U. S. Geological Survey).

A

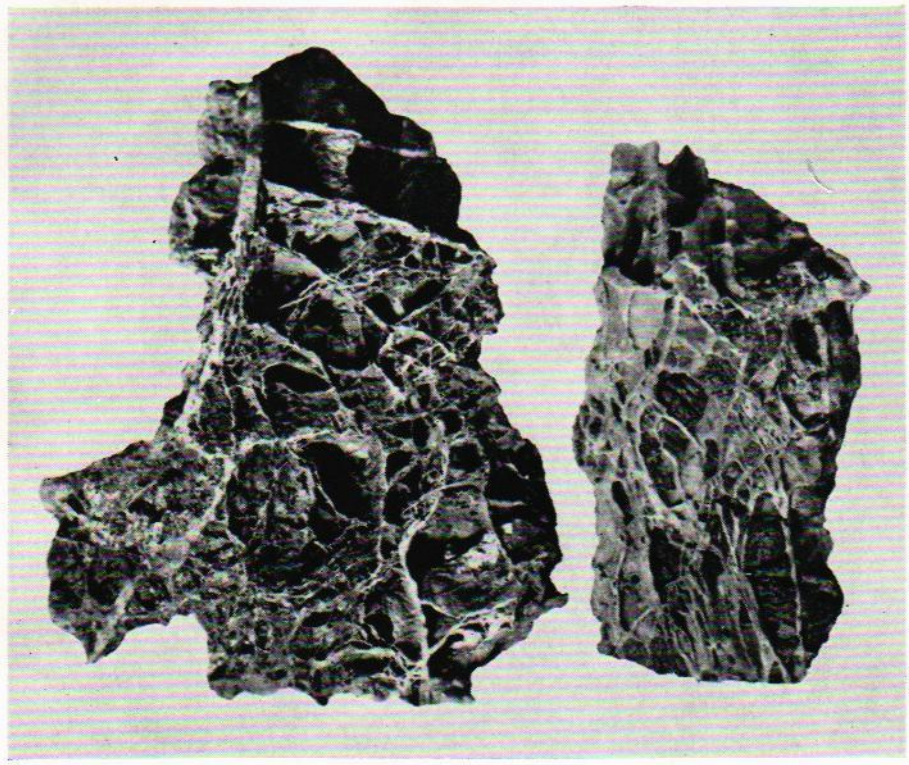

B

Plate 5

SILICA STRUCTURES

A. Hypogene silica boxwork, Calera, Chihuahua, Mexico. Scale × ¾.
B. Hypogene silica veinlets in sphalerite, Sonora, Mexico. Scale × ¾.

A

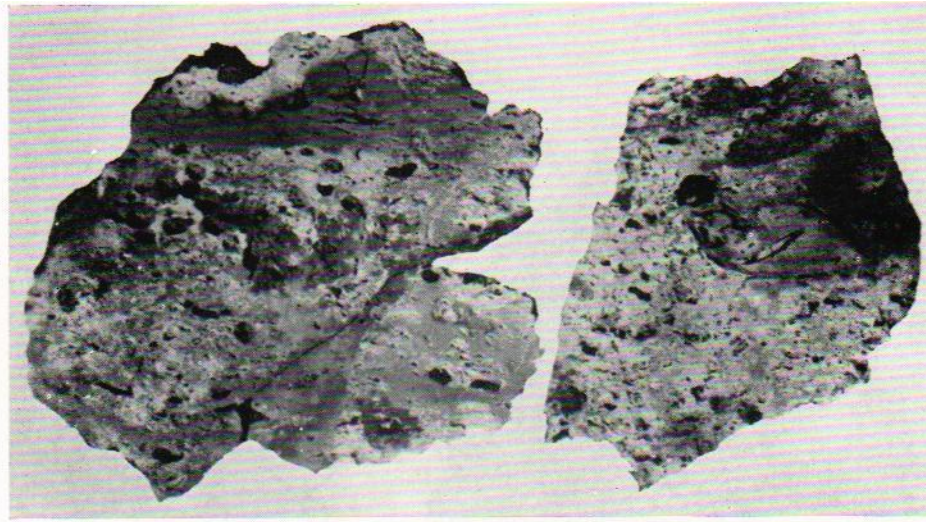

B

Plate 6

GOSSAN AND ORE, SHINGLE CANYON, NEW MEXICO

A. Flat cut surfaces of gossan, Shingle Canyon, New Mexico. Scale × 1.
B. A flat cut surface of zinc ore, Shingle Canyon, New Mexico. Scale × 1.

A

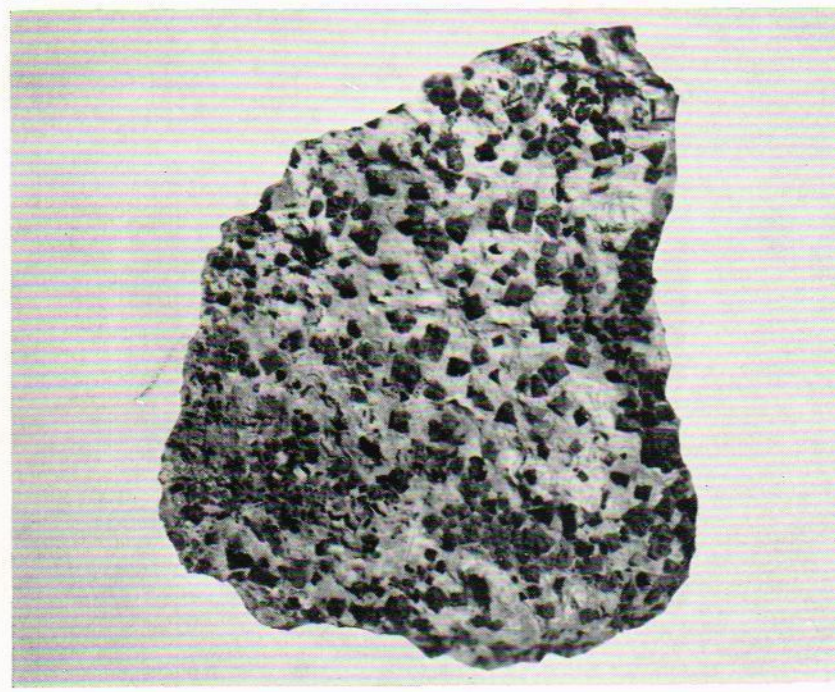

B

Plate 7

PEWABIC BOXWORKS AND GOSSAN

A. Goethite boxworks forming in magnetite, Pewabic quarry, Hanover, New Mexico. Scale × 1.
B. Pyrite gossan, Pewabic mine, Hanover, New Mexico. Scale × 1.

Index